Chapter V

Continuum Topology Optimization Problems, Results and Discussions

Topology optimization finds the optimal layout of a structure within the given domain. There are many studies of the topology optimization in mechanical engineering such as solids mechanics [72]-[81], heat transfer [82]-[84], fluid mechanics [22], [85], and multi-displinary problems [86]-[88]. As previously described in Chapter I, the topology optimization may be divided into 3 main categories – the discrete truss design, unit cell properties, and continuum topology optimization. The purpose of the continuum topology optimization is to allow the creation of new boundaries. The space that contains the structure is specified and divided into a number of grids; different configurations are obtained by selective filling these grids or leaving the space empty.

Various methods were proposed for continuum topology optimization in the last twenty years. Many continuum topology optimization problems are solved by sensitivity analysis methods such as [16], [17], [19]-[23], [72], [78], [82], [84], [88]-[95]. This method can be generally described as follows. Firstly, an initial structure is used to evaluate sensitivity results, which are derivative values. Then during optimization, a decision variable, representing an element of the domain is changed according to the sensitivity analysis results in order to obtain an updated structure. The sensitivity results of the updated structure are evaluated again; this process is continuously repeated until the terminated condition is satisfied. The sensitivity analysis method is simple to implement. However, it is quite hard to compute the sensitivity values in practical topology optimization problems, due to the difficulties in formulating objective functions or design constraints as explicit mathematical formulations expressed with decision variables, especially for problems with complex boundary conditions or non-linear problems [25]. In addition, many previous studies such as [16], [17], [19], [24], [25], [74] ,[83],

[87] employ density methods which necessarily encode a decision variable by a real number, whose value is between 0 and 1, representing the material density of its corresponding element, as optimizers. A density decision variable by this encoding is artificial as a physically meaningful decision variable must be either 0 or 1. Therefore, it is necessary to deal with material density elements after an optimized structure is obtained [96].

The density methods are quite simple in applications, they are attractive to engineers. However, they have the lack of theoretical support on the relationship between the density and the material properties [25]. Due to these drawbacks of this optimization, a discrete decision variable, of which value is either 0 or 1, is more practical. Optimizers using the discrete decision variable do not have such problems; they are more suitable than the density methods. However, the discrete decision variable may cause difficulties derivative-based optimizers.

A genetic algorithm (GA) is well-suited to continuum topology optimization problems, since it does not need explicit mathematical expressions for objective functions and constraints as well as can deal with problems that are hard to solve by sensitivity analysis methods. It can encode a structure directly into a binary string, of which a bit is represented by 0 or 1. In addition, it can be used to solve multi-material structural topology optimization such as [97], [98]. For a problem in which a structure is constructed by two types of materials, it encodes a structure into a tri-nary string where 0 represents an empty element, 1 represents an element filled with the first type of material, and 2 represent for an element filled by second material. Compared to sensitivity methods, there are only a few studies such as [99]-[105] which employ GA as the optimizer for continuum topology optimization problems.

In many previous studies, the problems are solved by single-objective optimizers in order to obtain one optimum solution by optimizing only one selected objective while other objectives are considered as problem restrictions

[15], [89], [93], [106]-[108] or using aggregative method (Figure 2.6) to transform multiple design objectives into one objective [109]-[112]. Actually, all design objectives of the problems should be optimized; Pareto-based multi-objective optimizers which employ the Pareto domination in Definition 2.1 in order to obtain multiple non-dominated solutions (Figure 2.7) are certainly more suitable than the uses single-objective optimizers.

In practice, there are many objectives to be designed for most continuum topology optimization problems. Previous studies in multi-objective continuum topology optimization problems that solve problems by Pareto-based multi-objective optimizers such as [34], [113]-[115] are focused on optimization of only 2-3 objectives and do not employ the Pareto domination with goal attainment [40], described by the equations (2.21)-(2.24). In addition, constraints of topology optimization problems such as compliance, structural weight, and number of holes or enclosed boundaries in a structure, can be considered as design objectives. All design objectives should be solved by multi-objective optimizer using the Pareto domination with goal attainment in which problem constraints can be treated as goals of the problems. By considering problem constraints as design objectives, there are many optimized objective for the problems. Therefore, multi-objective evolutionary algorithms (MOEAs) which are developed for optimization problems with many objectives such as improved compressed-objective genetic algorithm (COGA-II) and co-operative co-evolutionary improved compressed-objective genetic algorithm (CCCOGA-II) are suitable for such problems.

This thesis will use 5 MOEAs, which were empirically studied by benchmark problems in the previous chapter, and finite volume method (FVM) to solve continuum topology optimization problems. The employed problems are a heat conduction problem, a linear-elastic problem, and a thermo-elastic problem, which can be considered a multi-displinary problem. The numbers of objectives for the heat conduction problem are 3-6, while those of the linear-elastic problem

and the thermo-elastic problem are 2-5. The performances of these MOEAs are evaluated to guarantee that the proposed MOEAs – co-operative co-evolutionary multi-objective algorithm (CCMOA), improved compressed-objective genetic algorithm (COGA-II), and co-operative co-evolutionary improved compressed objective genetic algorithm (CCCOGA-II) are not only suited to solve well-established benchmark problems but also for multi-objective continuum topology optimization problems. Subsequently, they may be useful for mechanical engineers in continuum topology optimization of practical problems.

5.1. Overview of Test Problems

This thesis studies 3 continuum topology optimization problems involving heat conduction, linear elastic, and thermo-elastic problems. In each problem, 4 sub-problems with different numbers of design objectives are considered; the numbers of objectives in the heat conduction optimization problem vary from 3-6, while those of the linear-elastic and thermo-elastic problems vary from 2-5. The descriptions of objectives and employed topology optimization problems are as follows.

5.1.1. Objectives

The objectives can be categorized into the basic and geometrical objectives. The numbers of basic objectives in the heat conduction, linear-elastic and thermo-elastic are 3, 2, and 2 respectively. The numbers of 3 additional geometrically structural objectives are used to makeup the required numbers. The variation of number of objectives can be represented by a topology optimization problem with m basic objectives, which implies that numbers of objectives are m to $m+3$. By optimizing only its basic objectives, the number of objectives is equal to m. The objective number is increased to $m+1$ by adding the first additional objective, and will be $m+2$, after the second additional objective is added and so on.

5.1.1.1. Basic Objectives

The basic objectives can be considered as particular performances of structures for a continuum topology optimization problem without concerning structural geometry. For example, the basic objectives can be weight, compliance, maximum stress, and maximum strain of an elastic problem. The basic objectives of all continuum topology optimization problems – heat conduction, linear-elastic, and thermo-elastic problems – in this thesis will be described in descriptions of the problems in the topic 5.2.

5.1.1.2. Additional Objectives

Optimal structures which are obtained from topology optimization require further interpretation and simplification for shape and sizing design [6]. The optimal structures with few large holes, smooth perimeter are preferred for subsequent interpretation and detailed design. Therefore, number of holes, hole area, hole perimeter, and total structure perimeter (holes plus outer boundary) should be considered as design objectives. Thus, 3 additional objectives, minimized objectives, are evaluated from these designed values.

The objectives can be described by an example of a structure, which is presented by shaded region, constructed in the domain of 20 × 12 grids as shown in the following Figure 5.1.

The first additional objective is the number of holes. For the structure in Figure 5.1, it is equal to 4.

The second additional objective, which indicates the structural smoothness, is the ratio of structural perimeter to structural area (R_{pa}). The perimeter of the structure (P_s) is equal to sum of the outer perimeter, P_0, and hole perimeters, C_1-C_4. Thus, P_s is equal to $P_0 + C_1 + \ldots + C_4$. The structural area A_s is the area of grey region or the material area. Therefore, the second additional objective of a structure is generally given by

$$R_{pa} = \frac{P_0 + \sum C_j}{A_s} \tag{5.1}$$

where C_j is the perimeter of a hole j. Figure 5.2 shows comparison of 2 structures in the domain with bad and good values of R_{pa}.

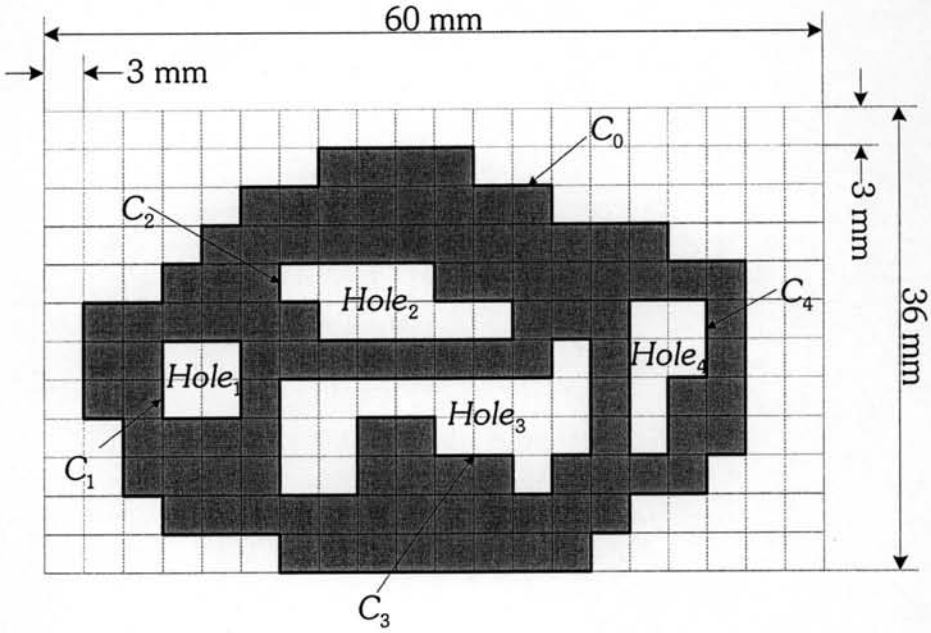

Figure 5.1 A structure in domain 20 × 12 grids.

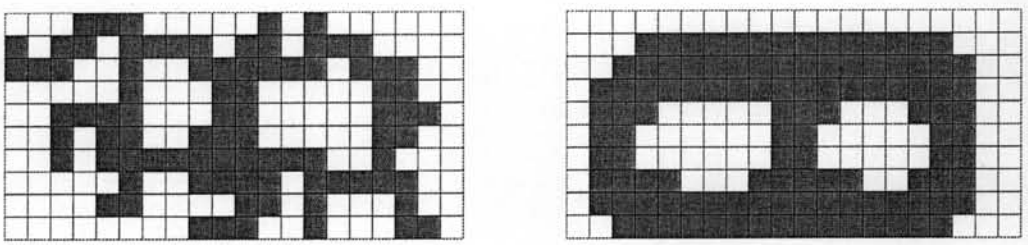

(a) R_{pa} = 407.0 m^{-1} (b) R_{pa} = 262.9 m^{-1}

Figure 5.2 Comparison of structures with (a) bad R_{pa} and (b) good R_{pa}.

The third additional objective, maximum value of ratios of hole perimeter to hole area (MRH_{pa}) which indicates smoothness of holes, is given by

$$MRH_{pa} = \max_j \left(\frac{C_j}{AH_j} \right) \tag{5.2}$$

where AH_j is area of hole j. For a structure with no holes, the third additional objective, MRH_{pa} of the structure is equal to zero. Figure 5.3 show comparisons of 2 structures with bad and good values of MRH_{pa} in the domain.

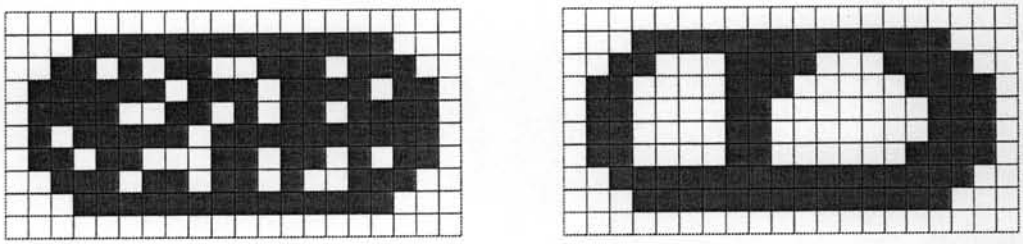

(a) $MRH_{pa} = 1333.3\ m^{-1}$ (a) $MRH_{pa} = 315.8\ m^{-1}$

Figure 5.3 Comparison of structures with (a) bad MRH_{pa} and (b) good MRH_{pa}.

5.2. Problems Descriptions

The descriptions of all employed problems will be illustrated as follows.

5.2.1. Heat Conduction Topology Optimization Problem

2D heat transfer problem with the convective boundary is used as the case study (Figure 5.4). The domain of this problem is a 1m-thick space of size 50 × 50 mm. In this thesis, the domain is divided into 5 × 5 grids, 10 × 10 grids, and 20 × 20 grids. Therefore, chromosome lengths are 25, 100, and 400 for domains with 5 × 5 grids, 10 × 10 grids, and 20 × 20 grids respectively.

Structures are intended to be lightweight configurations that transport heat from a point source Q at a bottom corner to a thin heating plate placing over the domain such that the temperature in the plate is evenly distributed. A structure has one fixed material element, which is shown by the grey element in Figure 5.4. The bottom surface of the element transfers the heat Q into the structure. There are 3 basic design objectives which are minimized structural weight, maximized average temperature $\bar{T}$ and minimized temperature standard deviation SD_T in the plate.

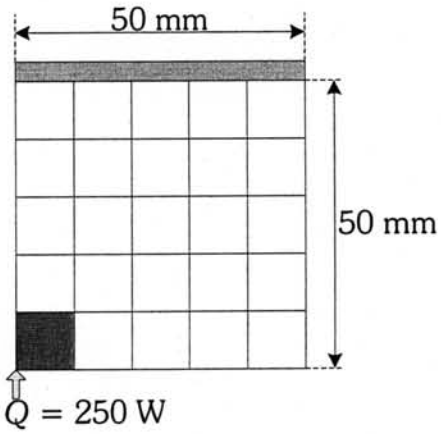

Figure 5.4 The heat conduction problem.

In the problem, structures are constructed by AISI C1020 steel of which thermal conductivity k is 46.73 W/mK [117], heat transfer coefficient h and ambient temperature, T_∞, are 25 W/m^{2}K and 0°C, respectively. The description of all design objectives of the problem is conclusively shown in Table 5.1.

Table 5.1 Description of design objectives of the heat conduction problem

Objectives		Description
Basic	1	Minimizing weight of a structure (solution)
	2	Maximizing average temperature of the plate($\bar{T}$)
	3	Minimizing temperature standard deviation SD_T in the plate
Geometry	4	Minimizing number of holes in the structure
	5	Minimizing ratio of structural perimeter to structural area (R_{pa})
	6	Minimizing maximum value of ratios of hole perimeter to hole area (MRH_{pa})

By the Pareto domination without goal attainment in Definition 2.1, there are two known extreme true Pareto-optimal solutions which are shown in Figure 5.5. The numbers in the square bracket are their values of all 6 objectives – weight (% of entire domain), $\bar{T}$ (°C), SD_T (°C), number of holes, R_{pa} (m^{-1}), and MRH_{pa}(m^{-1}). The first solution (Figure 5.5a) has least weigth which is the best first objective and equal to 5% of entire domain. The second solution (Figure 5.5b)

has maximum weight (100% of entire domain) which is the worst first objective, and maximum $\bar{T}$ (48.21°C) which is the best second objective.

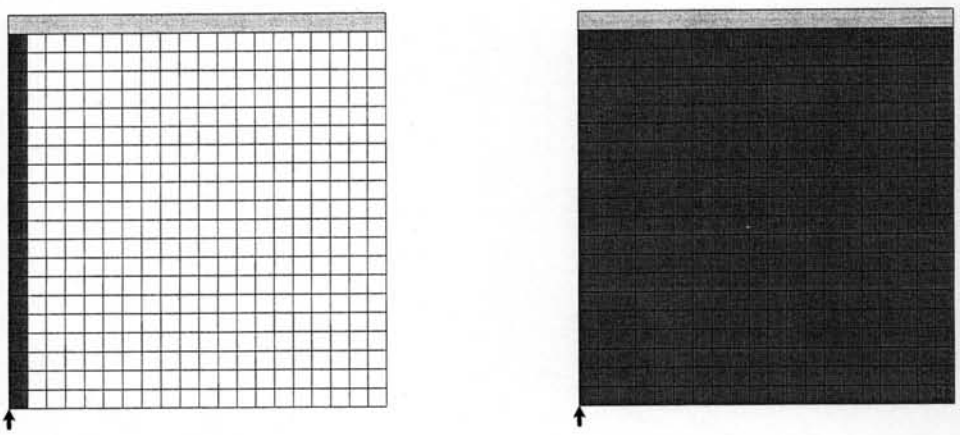

(a) [5.0, 31.15, 4.67, 0, 840.0, 0.0] (b) [100.0, 48.21, 0.20, 0, 80.0, 0.0]

Figure 5.5 Two known extreme true Pareto-optimal solutions of the heat condution problem.

However, these two known extreme true Pareto-optimal solutions may not be useful in particular way because the first solution has very poor third objective (SD_T) while the second solution has very poor first objective (structural weight). Therefore, other non-dominated solutions that are more useful than these two solutions are necessary for the problem.

5.2.2. Linear-Elastic and Thermo-Elastic Topology Optimization Problems

A simply support plate subjected to concentrated force and thermal loadings [71] (Figure 5.6), is used as the test cases for linear-elastic and thermo-elastic topology optimization problems. These plane-stress problems have the 1m-thick domain of size 400 × 100 mm. The domain is divided into 20 × 5 grids and 40 × 10 grids. Figure 5.6 shows the divided domain of 40 × 10 grids. Due to symmetry of the domain as shown in Figure 5.6, the corresponding coded chromosome lengths of the problems are 50 (10 × 5) and 200 (20 × 10) bits for half domains with 20 × 5 and 40 × 10 grids, respectively.

The plate is subjected to concentrated and thermal loads. There are 4 fixed material elements of divided domains, in Figure 5.6 the fixed elements are represented by gray elements; two elements surrounding the concentrated force and two elements on the supports. A concentrated load P = 1.0 MN, is applied at the center of the bottom surface in which the ambient temperature, T_∞, and convection coefficient are 0°C and 120 W/m^{2}K respectively. The material used for the problems is the steel AISI 304 of which Young elastic, E, Poison's ration, ν, thermal expansion coefficient, α, and thermal conductivity, k, are 193 GPa, 0.29, 17.82 μ/°C, and 16.27 W/mK [117], respectively. The temperature boundary surface with constant temperature, T_0, causing thermal load into the plate is displayed by the horizontal dash line as shown in Figure 5.6. There is no thermal load for the linear-elastic problem in which the temperature T_0 is then equal to the ambient temperature T_∞. In the other hand, three values of T_0 – 10°C, 20°C, and 40°C – are used for the thermo-elastic problem.

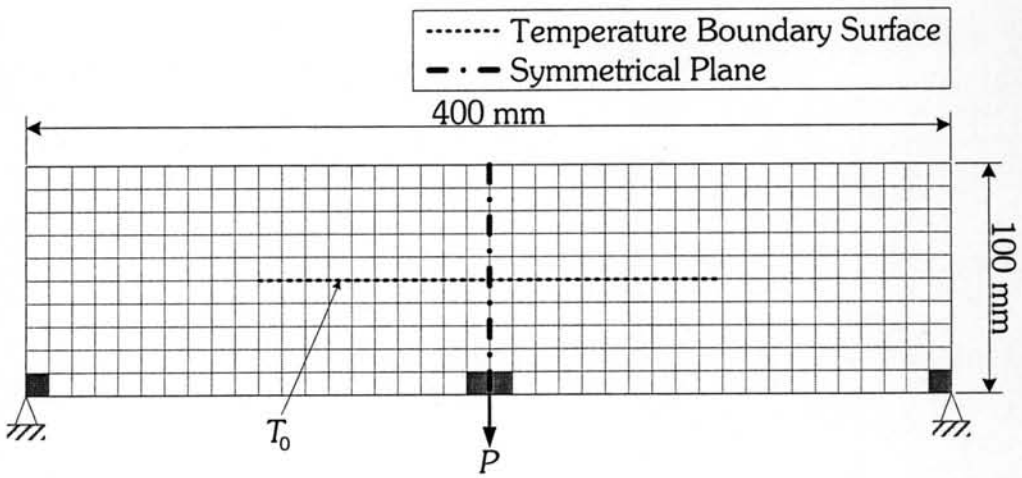

Figure 5.6 The linear-elastic and thermo-elastic topology optimization problems.

There are two design basic objectives for this problem of which the first objective is the minimized weight and the second objective is the minimized compliance, Π, which is given by

$$\Pi = \int_V \frac{E}{1-\nu} \alpha T u_{i,i} dV + \int_S t_i u_i dS \tag{5.3}$$

where T, u_i, and t_i denote temperature field, displacement field, and surface force. The description of all design objectives of the linear-elastic and thermo-elastic problems are shown in Table 5.2.

Table 5.2 Description of design objectives of the linear-elastic and thermo-elastic problems

Objectives		Description
Basic	1	Minimizing weight of a structure (solution)
	2	Minimizing compliance, Π, of the structure
Geometry	3	Minimizing number of holes in the structure
	4	Minimizing ratio of structural perimeter to structural area (R_{pa})
	5	Minimizing maximum value of ratios of hole perimeter to hole area (MRH_{pa})

By the Pareto domination without goal attainment in Definition 2.1, there are two known extreme true Pareto-optimal solutions which are shown in Figure 5.7 for the linear-elastic problem. The numbers in the square bracket are their values of all 5 objectives – weight (% of entire domain), Π (N·m), number of holes, R_{pa} (m^{-1}), and MRH_{pa} (m^{-1}). The first solution (Figure 5.7a) has least weigth, the best first objective, which is equal to 10% of entire domain. The second solution (Figure 5.7b) has maximum weight (100% of entire domain) which is the worst first objective, and minimum compliance Π (63.3 N·m) which is the best second objective.

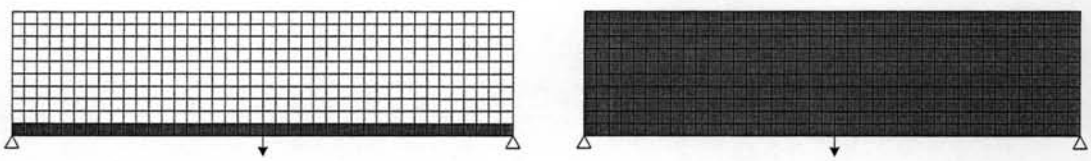

(a) [10.0, 30374.7, 0, 205.0, 0.0] (b) [100.0, 63.3, 0, 25.0, 0.0]

Figure 5.7 Two known extreme true Pareto-optimal solutions of the linear-elastic problem

On the other hand, by the Pareto domination without goal attainment in Definition 2.1, only one known extreme true Pareto-optimal solution is known in the thermo-elastic problem for any values of T_0. It is the same as the first known extreme true Pareto-optimal solution of the linear-elastic problem in Figure 5.7a. It has no elements contacting temperature surface boundary, it is not subjected to thermal load and is subjected to only mechanical load as the linear-elastic problem. For any value of T_0, objectives the known extreme true Pareto-optimal solution for the thermo-elastic problem are the same as those of the linear-elastic which are displayed in the square bracket in Figure 5.7a.

Similar to the heat conduction problem, the known extreme true Pareto-optimal solutions may not be actually useful for the linear-elastic and thermo-elastic problems. The extreme true Pareto-optimal solution in Figure 5.7a has very poor second objective (compliance, Π) for the linear-elastic and thermo-elastic problems while that in Figure 5.7b has very poor first objective (structural weight) for the linear-elastic problem. Other non-dominated solutions that are more useful than these two solutions are therefore necessary for the problems.

Figure 5.8 shows optimal structures, whose weights are 30% of the domain, obtained by design sensitivity analysis (DSA) [71] which employs an artificial decoded density decision variable. From the structures in Figure 5.8(a) and Figure 5.8(b), the mechanical loading has more impact than the thermal loading with the V-shaped material distribution. In the other hand, when the thermal loading with high temperature T_0, has more impact than the mechanical loading, the structure in Figure 5.8(c) has no elements that are in contact with the temperature surface (Figure 5.6) in order to eliminate the thermal loading.

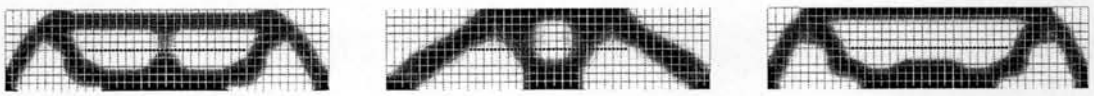

(a) No thermal load (b) High applied force (c) High thermal load

Figure 5.8 Optimal solutions for (a) no thermal load, (b) high applied force, and (c) high thermal load by the design sensitivity analysis (DSA) [71].

5.3. MOEA Operators for Continuum Topology Optimization

This section will present 6 MOEA operators – structural chromosome encoding, relevant structural calculation, initial population generation, progressive refinement run, objective increasing run, and performance matrix calculation – for the continuum topology optimization problems.

5.3.1. Structural Chromosome Encoding

For a domain which is divided into a number of grids, a structure within the domain is obtained by selective filling these grids or leaving the space empty. A structure is encoded into MOEA framework by a binary string or chromosome whose length is equal to the number of the divided grids. For a domain is divided into $N_r \times N_c$ grids where N_r and N_c are number of rows and columns respectively, a chromosome representing a structure can be described as follows. The first N_c bits of the chromosome representing the first row of the structure, the second N_c bits represents the second row and so on. To illustrate the encoding, Figure 5.9shows examples of chromosome encoding of two different structures, which are displayed by the shaded regions, in domains with 5×5 grids.

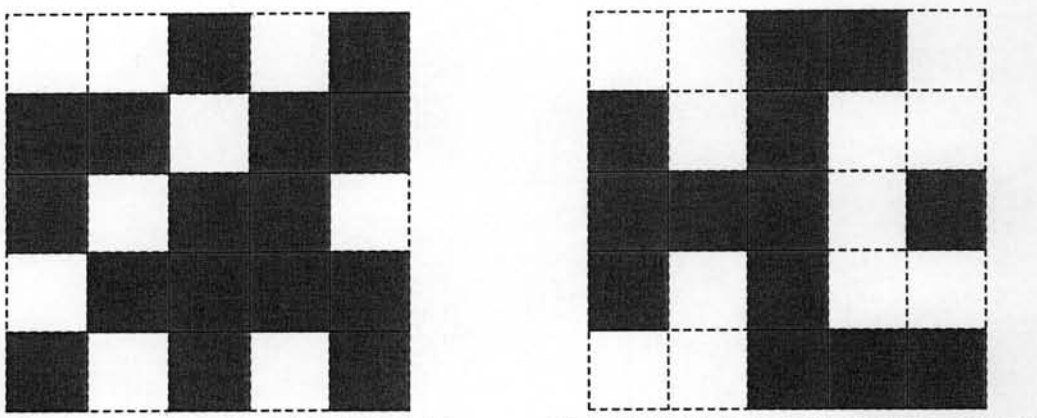

Figure 5.9 Chromosome encodings of two structures in domain with 5×5 grids.

5.3.2. Relevant Structural Calculation

Relevant structural determination for the objective calculation for all continuum topology optimization problems can be described using the heat conduction problem as an example. For an individual *i*, of which corresponding structure is shown in left-hand side of Figure 5.10, the stripped shaded blocks are useless material which are not in connection with others and necessary for objective calculation. On the other hand, the non-stripped grey blocks which connect the fixed structural element to the plate (Figure 5.10) are relevant material blocks. Thereafter, objectives of the individual *i* is evaluated by the structure without the useless blocks which is shown in the right-hand side of the figure.

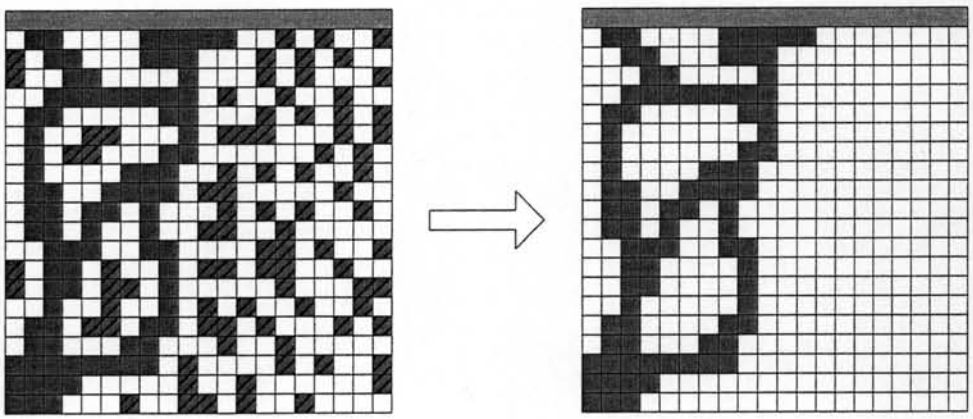

Figure 5.10 Objective calculation.

In addition, all topology optimization problems employed in this thesis have the minimized structural weight as the first objective. Compared to another individual with equal relevant material blocks, an individual having useless material blocks is, in fact, has a worst first objective. Therefore, the number of useless material blocks should be added in a comparison of any two individuals, when their calculated objectives are equal. Then, by the Pareto domination in Definition 2.1, they do not dominate each other. However, by the consideration of useless material blocks, the individual with the less number of useless material blocks considerably dominates the other.

5.3.3. Initial Population Generation

Unlike the benchmark multi-objective optimization problems in the previous chapter, a usual randomized individual may not appropriate for all topology problems. Initial population generation that can create an appropriate individual for a topology problem is necessary. The initial population generation for the employed problems is described as follows.

An individual in the initial randomized population should be customized to employed problems. The specified initial population generations are necessary for the employed problems. The appropriate individual is generated by taking into accounts of fixed elements of the problems. An appropriate individual of the heat conduction problem must have the connectivity between the fixed element, which transfers input heat into the structure and heating plate (Figure 5.4). Similarly, for the linear-elastic and thermo-elastic problems, an appropriate individual must have the connectivity between all 4 fixed material elements (Figure 5.6). The comparisons of inappropriate and appropriate individuals for the heat conduction problem with domain 20 × 20 grids, and linear-elastic and thermo-elastic problems with domain 40 × 10 grids are shown in Figure 5.11 and Figure 5.12, respectively. Due to symmetry in linear-elastic and thermo-elastic problems, only halves of the structures are shown in Figure 5.12.

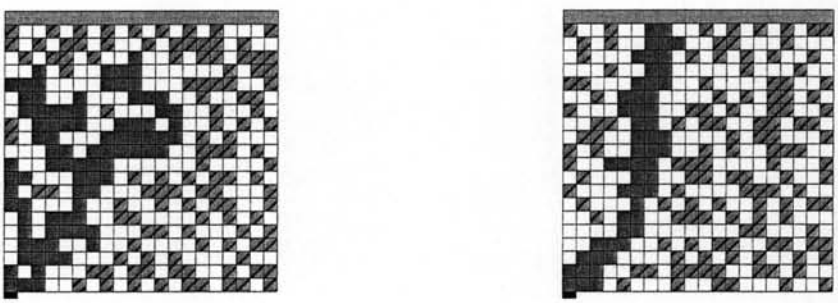

(a) (b)

Figure 5.11 An example of (a) an inappropriate individual and (b) an appropriate individual for the heat conduction problem.

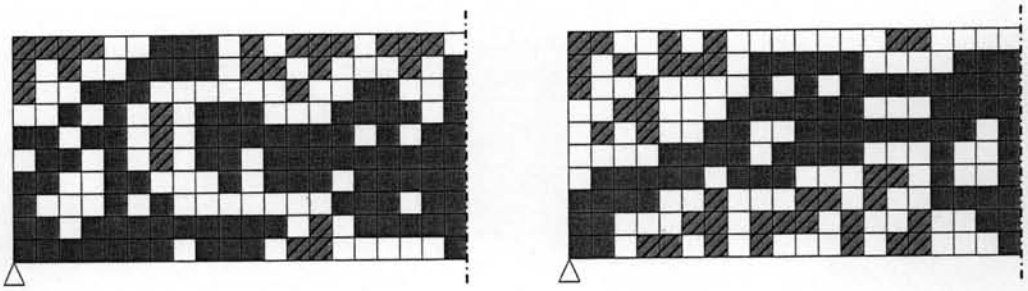

(a) (b)

Figure 5.12 An example of (a) an inappropriate individual and (b) an appropriate individual for the linear-elastic and thermo-elastic problems.

The generation of a randomized appropriate individual can be described as follows. At first, after a randomized individual is initially created, it is then checked whether it is appropriate or not. If it is inappropriate, only useless material and empty elements are re-randomized to obtain another individual which is checked again. This generation process is then repeated until an appropriate individual is obtained. The examples of randomized individual generations for the heat conduction, and linear-elastic and thermo-elastic problems are shown in Figure 5.13 and Figure 5.14, respectively. In the figures, simple grey blocks are appropriate material elements while stripped shaded blocks are inappropriate material elements.

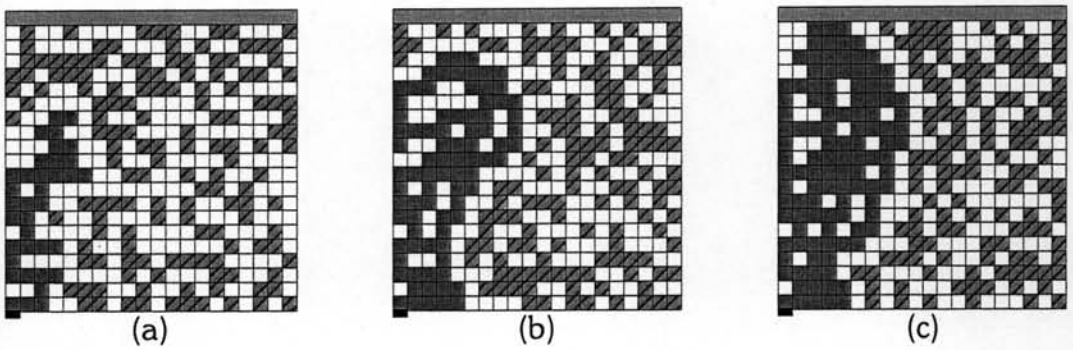

(a) (b) (c)

Figure 5.13 An example of the successive generation of randomized individuals for the heat conduction problem.

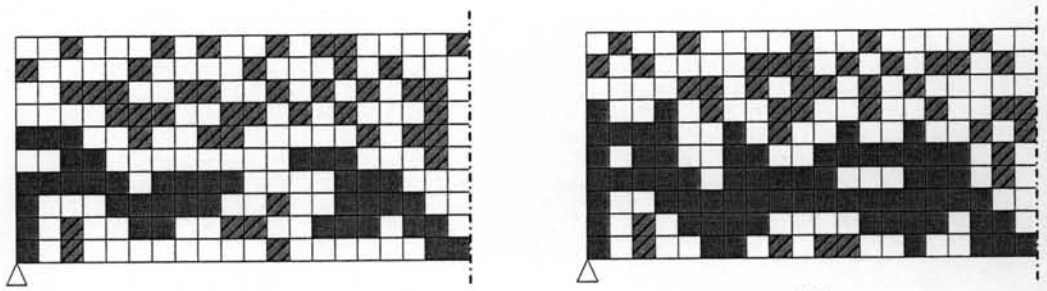

(a) (b)

Figure 5.14 An example of the successive generation of randomized individuals for the linear-elastic and thermo-elastic problems.

For the heat conduction problem (Figure 5.13), the first randomly generated individual (Figure 5.13a) is inappropriate for the problem. Thereafter, the random generation must be repeated, for the remaining the appropriate elements, the other elements are repeatedly generated. However, the second generated individual (Figure 5.13b) is still inappropriate for the problem and the third generation will be necessary. After this generation, an appropriate individual (Figure 5.13c) is obtained; therefore this generated individual is an appropriate randomized individual and is a member of the initial population accordingly. Similarly, individual generation for the linear-elastic and thermo-elastic problems (Figure 5.14) uses only two successive generation processes.

In addition, a researcher can add some preferred individuals into the initial population of a problem but, no preferred individuals are added into initial population of any employed problems in this thesis.

Nonetheless, inappropriate individuals may arise during the searching process. Therefore, a minimized objective and a maximized objective of these individuals are simply set to the bad values of ∞ and $-\infty$, respectively.

5.3.4. Progressive Refinement Run

This thesis employs a progressive refinement run [116], which was proposed for single-objective topology optimization problems, for the employed

continuum topology optimization problems. It uses a number of running stages in which divided domains is coarsest in the first running stage and finest in the final running stage. Thereafter, the chromosome length, which equal to the number of elements in the designed domain, is increased with the running stage. The domain in the second running stage is discretized by dividing an element of the previous stage into 2 × 2 grids and quadrupling chromosome length. For a problem of which the domain is divided into 5 × 5 grids in the first running stage, then domains with 10 × 10, and 20 × 20 grids are used in the second and third running stages, respectively (Figure 5.15).

Figure 5.15 Divided domains of (a) first stage, (b) second stage, (c) third stage.

Compared to runs that use only the final stage domain for the optimization, the progressive refinement run can exponentially reduce search space in early running stages of the problem. If only the finest grid in the final stage is used in entire run, the number of possible solutions is $2^{400} \approx 2.58 \times 10^{120}$. However, in the progressive refinement run, the number of possible solutions are only $2^{25} \approx 3.36 \times 10^{7}$ and $2^{100} \approx 1.27 \times 10^{30}$ in the first and second stage respectively.

The procedure of the progressive refinement run is described by Figure 5.16. At first, population in the first running stage domain is randomly generated and minimum numbers of all running stage, *MG*, are defined. Stage counter, *i*, and generation counter, *j*, of the running stage are all set to 1. The population is evolved by an MOEA process as the generation counter *j* is increased by 1. The

generation counter, j, is increased until j is more than minimum numbers of generation of stage i or MG_i, and solutions are converged. Thereafter the stage counter i is increased by 1 and generation counter j of the next running stage is initially set to 1. Initial population and archive in updated stage is generated by those of previous stage. This generation will be described latter. The procedure is repeated until generation counter j of final stage i is more than minimum number of generation of the final stage, MG_i, and solutions in the final stage are converged. The non-dominated solutions of the final archive of an MOEA with archive or those of the final population of an MOEA without archive are output of the progressive refinement run.

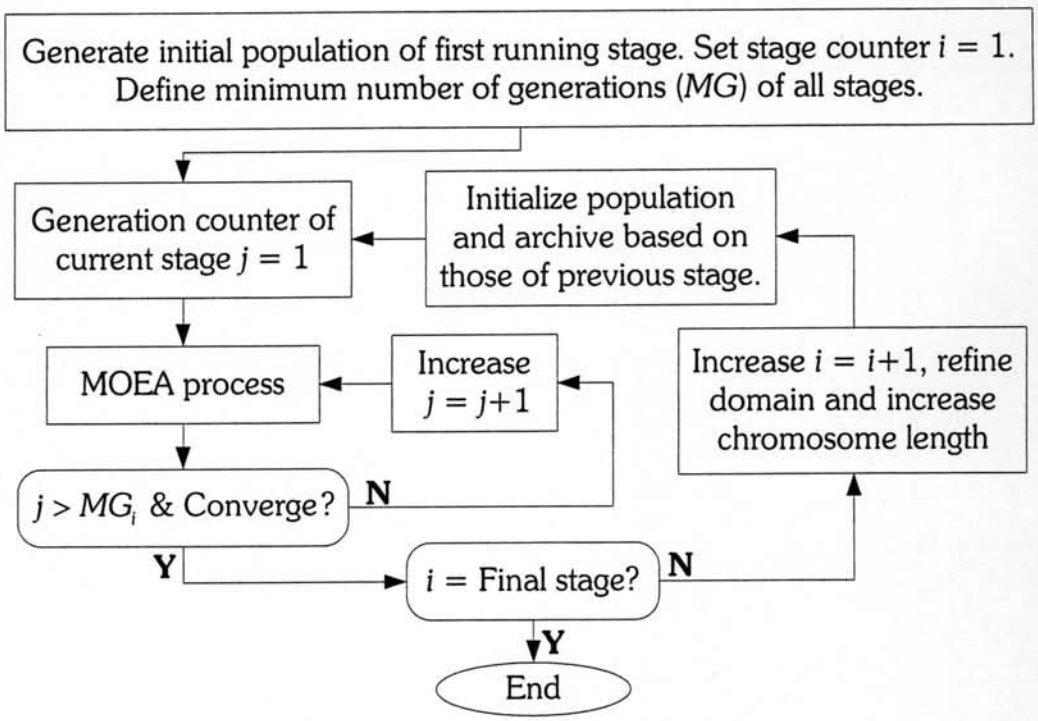

Figure 5.16 Procedure of domain refinement run.

The solution convergence can be described as follows. Given **A** and **B** are sets of solutions of the population (NSGA-II) or the archive (SPEA-II, CCMOA, COGA-II, CCCOGA-II), in the current generation and those in the k^{th} previous generation respectively, where k is arbitrary. If k is equal to 10 and **A** is the set of solution in the current 100^{th} generation, then, **B** is the set of solution in the 90^{th}

generation. The converged condition of solutions is simply given by the following inequality

$$C(\mathbf{A},\mathbf{B}) \leq C(\mathbf{B},\mathbf{A}) \tag{5.4}$$

where $C(\mathbf{A}, \mathbf{B})$ is the coverage of the solution set **A** over the solution set **B** while $C(\mathbf{B}, \mathbf{A})$ is the reverse of $C(\mathbf{A}, \mathbf{B})$. The solution set coverage, C, which was proposed by Zitzler et al. [38], is used to compare any two non-dominated solution sets. It is mathematically defined by

$$C(X',X'') = \frac{\left|\{\mathbf{a}'' \in X''; \exists \mathbf{a}' \in X' : \mathbf{a}' \preceq \mathbf{a}''\}\right|}{|X''|} \tag{5.5}$$

where $\mathbf{a}' \preceq \mathbf{a}''$ mean $\mathbf{a}'$ covers $\mathbf{a}''$ ($\mathbf{a}'$ dominates or equals $\mathbf{a}''$) and $C(X',X'') \in$ [0, 1]. $C(X',X'') = 1$ means that all solutions in X'' are dominated or equal to solution in X'. For the other extreme value, $C(X',X'') = 0$ represents the situation in which none of the solution in X'' are covered by the set X'. If $C(X',X'') > C(X'',X')$, it can say that the solution set X' is better than the set X'' according to the coverage definition. By this discussion, the equation (5.5) shows that the solution set **A** of the current generation is worse than or equal to the solution set **B** of the k^{th} previous generation.

The generation of the initial population and archive of a running stage $i \geq 2$ will be described as follows. At the beginning, for an MOEA with archive, a certain number of elitist solutions in the final archive of the previous running stage i-1 are added into the initial archive. The addition of the elitist solutions is as follows. Non-dominated solutions in the archive of the previous running stage i-1 are moved into the initial archive of running stage i. If the number of the non-dominated solutions is more than the defined number of elitist solutions, some non-dominated solutions are truncated and put back into the final archive of the previous running stage. Similarly, for an MOEA without archive, a certain number of elitist solutions, in population of the previous running stage i-1 are added into

the initial population of the running stage i. After all elitist individuals are obtained, the other individuals in the initial population or archive are then one-by-one generated from their predecessor in the remaining final population or archive in the previous running stage. An example of an individual generation in a domain with 10 × 10 grids from its 5 × 5 grids predecessor is shown in Figure 5.17. An element in a generated individual is randomly generated by probability whether it will be material filled or empty. The probability is evaluated from the contacted elements of its corresponding element in the predecessor. The probability whether the element is filled or empty is equal to ratio of numbers of filled or empty contacted elements to the total number of contacted elements.

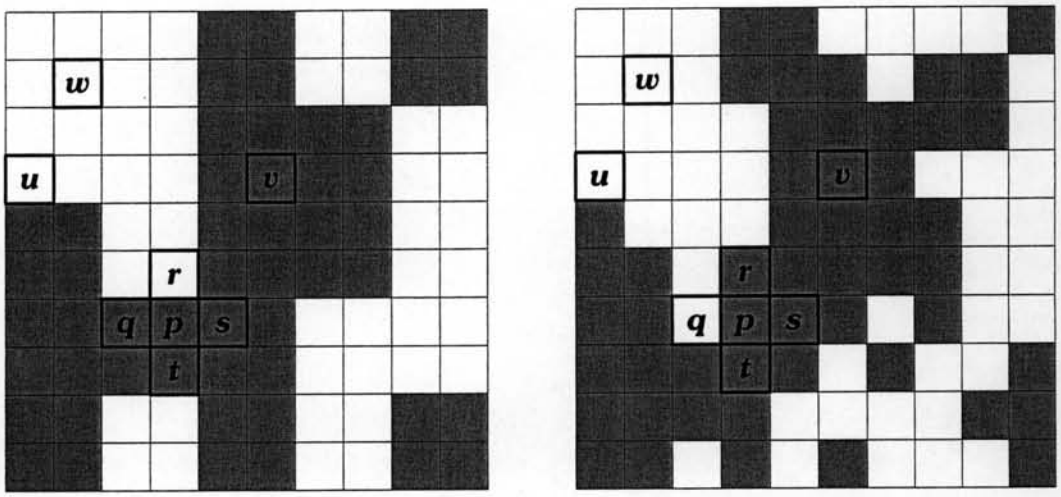

(a) Predecessor (b) Generated individual

Figure 5.17 An example of a predecessor (a) and (b) its successor individual in a domain with 10 × 10 grids.

For the predecessor in Figure 5.17(a), the element p has 4 contacted elements q, r, s, and t, of which 3 is filled and 1 empty. Therefore, the probabilities of the element p in the generated individual to be material filled and empty elements are equal to 3/4 and 1/4, respectively as shown in Figure 5.17(b). In the same way, the element u has only 3 contacted material, the probabilities are 1/3 and 2/3, respectively. By these generation probabilities, the elements v and w of the generated individual are certain to be filled and empty, respectively.

As previously stated, performance objectives of a structure is evaluated by the finite volume method (FVM). For the progressive refinement run, FVM uses domain discretization as the domain divisor in the final running stage for the objective evaluation of any running stage. The progressive refinement run with 3 running stages is used for the heat conduction problem, while 2 running stages for the linear-elastic and thermo-elastic problems.

5.3.5. Objective Increasing Run

Although the proposed MOEAs – COGA-II and CCCOGA-II – outperform the well-established MOEAs – NSGA-II and SPEA-II, values of M_1 deteriorate when the number of objectives is increased when the results of distances from true Pareto-optimal front, M_1, of the problems DTLZ1-7 in Table 4.6-Table 4.9 are studied. To reduce this degradation for multi-objective topology optimization problems, this thesis proposes the objective increasing run. Using only a few objectives to be optimized in the first run, the number of optimized objectives is then increased one-by-one to the required number of objectives.

The procedure of the run can be described in Figure 5.18. At the beginning, the progressive refinement run (Figure 5.16) by an MOEA is used to search for solutions by optimizing only 2-3 objectives and treating other objectives as problem constraints with the same as goals for these objectives to ensure that the goals for all employed topology optimization problems comply with the stated objectives in Table 5.4. Similar to an inappropriate individual, the minimized and maximized objectives of an individual which is unable to satisfy the problem constraints are simply set to ∞ and $-\infty$, respectively. After search solutions for the initial number of objectives are converged, the number of optimized objectives is increase by one while the remaining non-optimized objectives are again treated as the problem constraints. The final population and final archive from the search for previous number of optimized objectives are directly transferred into the initial population and initial archive in the next run

with the increasing number of optimized objectives. The running process is continuously repeated until the solutions in the run with all optimized objectives are converged. Similar to the progressive refinement run, solution convergence is tested when the number of generation is more than the arbitrarily defined minimum number of generations for a search of any number of objectives. The converged solutions of the run with all optimized objectives are therefore output of the objective increasing run. In addition, the objective increasing run can use more than one MOEA in runs for the numbers of optimized objectives, while the progressive refinement run (Figure 5.16) is used only for the initial number of objectives.

Orders of objectives for the objective increasing run of the heat conduction, and linear-elastic and thermo-elastic problems are the same as those in Table 5.1 and Table 5.2, respectively.

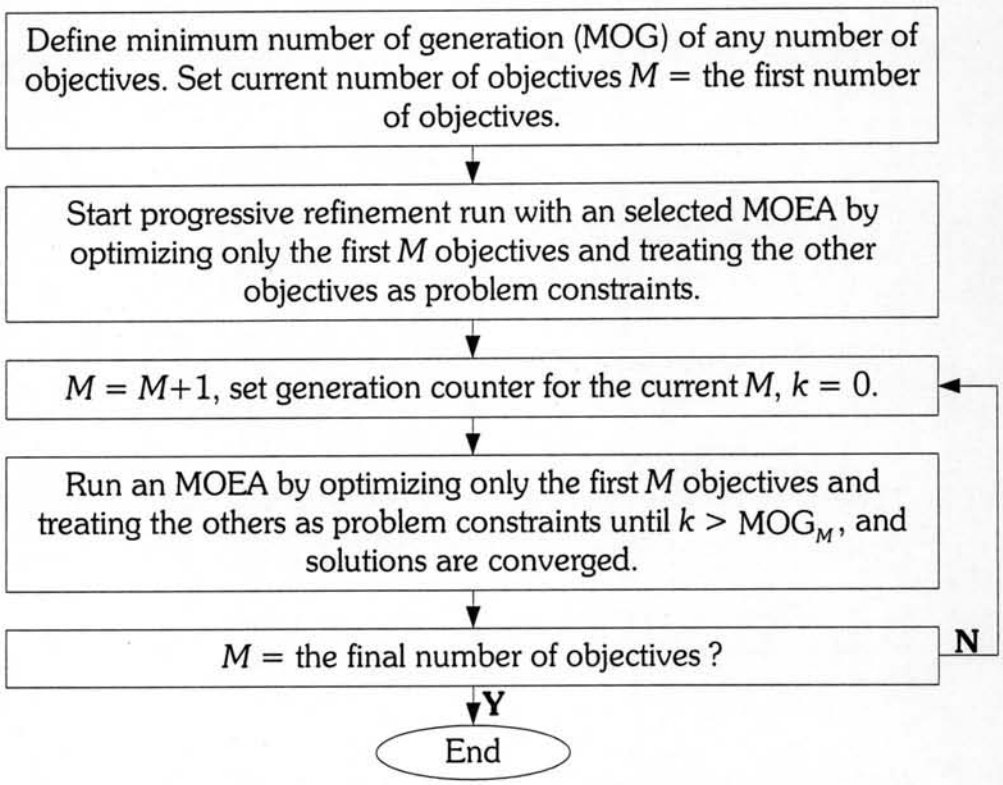

Figure 5.18 Objective increasing run.

5.3.6. Performance Metric

The performance objectives of an individual are numerically evaluated by the finite volume simulation. However, there are many possible configurations for each problem, the least number of possible configurations, which of a heat conduction problem with the domain of 20×20 grids, is equal to $2^{400} \approx 2.58\times10^{120}$. The true Pareto front of the problem can only be generated by an exhaustive search. Due to limitation of time, it is impossible to evaluate objectives of all possible configurations in order to obtain the true Pareto front. Similar to the linked DTLZ problems, artificial true Pareto optimal front obtained from the non-dominated individuals of merged individuals of all runs is used instead of the true Pareto front. Similar to evaluation of M_1 in previous chapter, a distance of a solution i to true Pareto-optimal front, d_i, the Euclidean distance of the solution i to its nearest solution j on the artificial true Pareto-optimal front, is evaluated by the following equation.

$$d_i = \sqrt{\sum_{k=1}^{m}\left(\frac{f_{ik} - f_{jk}}{(f_k)_{\max} - (f_k)_{\min}}\right)^2} \tag{5.6}$$

where f_{ik} and f_{jk} are objectives k of solutions i and j, respectively. The $(f_k)_{\min}$ and $(f_k)_{\max}$ are minimum and maximum value of an objective k of the artificial true Pareto-optimal solutions. The criterion M_1 of a non-dominated solution set is equal to the average of d_i of non-dominated individuals in the set. For the diversity criterion, the results of clustering index (CI) of the benchmark problems in pervious chapter are considered good enough to show diversity of obtained solutions by employed MOEAs. In addition, it is not necessary to evaluate performance of employed MOEAs by direct comparisons of solutions, which use many comparing times, and it is hard for the direct comparisons of solutions in an optimization problem with more than 2 objectives. The criterion M_1 is quite acceptable and easy to evaluate performances of MOEAs. Therefore, only the

criterion M_1 is necessary for the comparison of performance of all employed MOEAs for all employed continuum topology optimization problems.

The following topic will display simulation results and discussions of continuum topology optimization problems which are employed in this thesis.

5.4. Simulation Results and Discussions

The progressive refinement and objective increasing runs are not used for comparison of all employed MOEAs. The domains for the comparison of the employed MOEAs are divided into 20 × 20 grids, and 40 × 10 grids for the heat conduction, and linear-elastic and thermo-elastic problems, respectively. The chromosome length in the heat conduction problem is 400. While due to symmetry of a structure, the chromosome length for linear-elastic and thermo-elastic problems is 200.

5.4.1. MOEA Settings

For co-operative co-evolutionary multi-objective algorithm (CCMOA) and co-operative co-evolutionary improved compressed-objective (CCCOGA-II), as described in Chapter II, a solution, which is a structure, is divided into several components or species. The numbers of species used for the heat conduction problem, and the linear-elastic and thermo-elastic problems are 5 and 10 respectively. Species arrangements for the problems are shown in Figure 5.19.

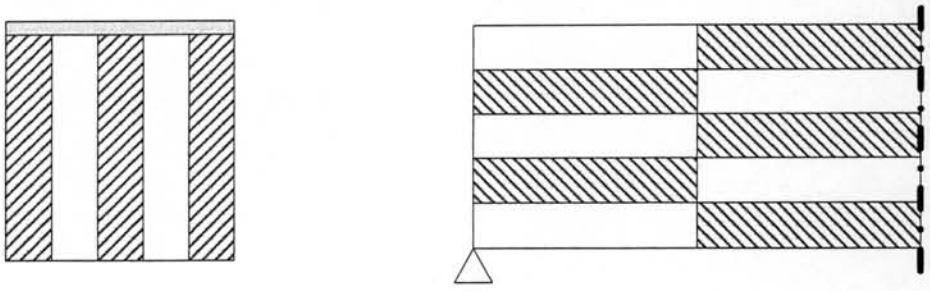

(a) (b)

Figure 5.19 Species arrangements in (a) the heat conduction and (b) linear-elastic and thermo-elastic problems.

The parameter setting for the employed MOEAs is shown in Table 5.3. For the thermo-elastic problem, only one value of temperature T_0 on the temperature surface (Figure 5.6), 10°C, is used for comparison.

Table 5.3 Parameter setting of the MOEAs for continuum topology optimization problems.

Parameter	**Setting and Value**
Chromosome coding	Binary chromosome with chromosome length of 400 (heat conduction problem), 80 (linear-elastic problem), and 200 (thermo-elastic problem)
Number of objectives	3-6 (heat conduction problem), 2-5 (linear-elastic and thermo-elastic problems)
Crossover method	Uniform crossover with probability = 0.9
Mutation method	Bit-flip polynomial mutation with probability = 0.02 (for NSGA-II, SPEA-II,COGA-II) and probability = 0.1 (for CCMOA, CCCOGA-II)
Population size	100
Archive size[1]	100
No. of generations	600
No. of repeated runs	10

[1]for SPEA-II, CCMOA, COGA-II, and CCCOGA-II.

Goals for design objectives in all problems are shown in Table 5.4; they are used for the Pareto domination with goal attainment [40] which is described by equations (2.21)-(2.24). The first objective of any problem, weight of a structure, is measured by percentage of material elements in domain. By the Pareto domination with defined goals in Table 5.4, it notes that no true Pareto-optimal solutions are known for any employed continuum topology optimization problems.

Table 5.4 Goals for all design objectives of continuum topology optimization problems.

Problems	**Heat conduction**	**Linear-elastic and Thermo-elastic**
Objective 1	≤ 50%	≤75%
Objective 2	≥ 30°C	≤ 600 N·m
Objective 3	≤ 0.75°C	≤ 5 holes
Objective 4	≤ 5 holes	≤ 200 m^{-1}
Objective 5	≤ 400 m^{-1}	≤ 200 m^{-1}
Objective 6	≤ 400 m^{-1}	–

For the continuum topology optimization problems, the criterion average distance to artificial true Pareto-optimal front (M_1), which is described in the topic 5.3.6, is used for comparing performances of all employed multi-objective evolutionary algorithms (MOEAs). Thereafter, progressive refinement and increasing objectives runs by selected MOEAs will be used to search non-dominated solutions of all problems – heat condution, linear-elastic and thermo-elastic problems.

Without concerning 3 geometrically structural objectives, the progressive refinement is used for the problems with only basic objectives. On other hand, the objective increasing run is used for the problem with all considered objectives. By the runs, solutions for two numbers of optimized objectives in each problem are displayed in thesis, where the numbers of optimized objectives are 3 and 6 for the heat conduction problem, and 2 and 5 for the linear-elastic and thermo-elastic problems.

The progressive refinement run (Figure 5.16) is used for optimizing basic objectives cases, while the objective increasing run (Figure 5.18) is used for optimizing all objectives cases. The orders of increasing objectives are the same as those in Table 5.1 for the heat conduction problem and Table 5.2 for linear-

elastic and thermo-elastic problems. The initial optimized objectives of the run are thus basic objectives of an employed topology optimization problem. There are 2 and 3 initial optimized objectives for the heat conduction, and linear-elastic and thermo-elastic problems, respectively.

Parameter settings of the progressive and objective increasing runs in all problems are shown in Table 5.5 and Table 5.6, respectively. Goals for design objectives in all problems in the progressive refinement and objective increasing runs are the same as those in Table 5.4.

Table 5.5 Parameter setting of the progressive refinement runs in continuum topology optimization problems.

Parameter	**Setting and Value**
Chromosome coding	Binary chromosome whose length is equal to number of divided elements in designed domain of each running stage
Numbers of objectives	3 and 2 for the heat conduction, and linear-elastic and thermo-elastic problems
Crossover method, mutation method, population size, and archive size	Same as in Table 5.3
Minimum number of generations in each running stage	50 for all running stage
k^{th} previous generation for convergence test	k = 40 for all running stage
Number of elitist individuals from previous stage	25% of population[1] or archive size[2]
No. of repeated runs	5

[1] for an MOEA without archive, [2] for an MOEA with archive

Table 5.6 Parameter setting of the objective increasing runs in continuum topology optimization problems.

Parameter	Setting and Value
Chromosome coding	Binary chromosome, chromosome length is equal to number of divided elements in designed domain
Numbers of objectives	6 and 5 for the heat conduction, and linear-elastic and thermo-elastic problems
Number of initial optimized objectives	3 and 2 for the heat conduction, and linear-elastic and thermo-elastic problems
Parameter setting of progressive refinement run for the initial optimized objectives	Same as in Table 5.5
Crossover, mutation methods, population size, and archive size	Same as in Table 5.3
Minimum number of generation for each number of optimized objectives	100 for all numbers of optimized objectives
Problem constraints due to remaining non-optimized objectives	Same as goals for the non-optimized objectives in Table 5.4
k^{th} previous generation for convergence test	k = 40 for all convergence test
No. of repeated runs	5

5.4.2. Overall results and Discussions

After the simulation run for the comparisons of all MOEAs – fast elitist non-dominated sortin genetic algorithm (NSGA-II), improved strength Pareto evolutionay algorithm (SPEA-II), co-operative co-evolutionary multi-objectivew algorithm (CCMOA), improved compressed-objective genetic algorithm (COGA-

II), and co-operative co-evolutionary improved compressed-objective genetic algorithm (CCCOGA-II) – for the employed continuum topology optimization problems, Comparisons of average (Avg) and standard deviation (SD) values average distance to artificial true Pareto-optimal front (M_1) of the MOEAs for the employed problems are shown in Table 5.7-Table 5.9, respectively.

Table 5.7 Comparisons of average (Avg) and standard deviation (SD) values of M_1 of the heat conduction problem.

Number of objectives		NSGA-II	SPEA-II	CCMOA	COGA-II	CCCOGA-II
3	Avg	0.1134	0.1415	0.2150	**0.0435**	0.0631
	SD	0.0529	0.0790	0.0808	0.0253	0.0659
4	Avg	0.0705	0.0834	0.1805	**0.0173**	0.0465
	SD	0.0216	0.0343	0.1007	0.0088	0.0335
5	Avg	0.1480	0.1240	0.1738	**0.0709**	0.0797
	SD	0.0581	0.0526	0.0485	0.0236	0.0376
6	Avg	0.1269	0.1156	0.1087	0.0798	**0.0568**
	SD	0.0346	0.0278	0.0276	0.0266	0.0250

Table 5.8 Comparisons of average (Avg) and standard deviation (SD) values of M_1 of the linear-elastic problem.

Number of objectives		NSGA-II	SPEA-II	CCMOA	COGA-II	CCCOGA-II
2	Avg	0.0111	0.0121	**0.0108**	-	-
	SD	0.0020	0.0036	0.0023	-	-
3	Avg	0.1001	0.1282	0.0880	0.0592	**0.0299**
	SD	0.0356	0.0372	0.0303	0.0333	0.0175
4	Avg	0.1057	0.1492	0.1122	0.0816	**0.0632**
	SD	0.0569	0.0498	0.0240	0.0429	0.0150
5	Avg	0.1819	0.1823	0.1561	0.0389	**0.0254**
	SD	0.1590	0.1252	0.0714	0.0129	0.0128

Table 5.9 Comparisons of average (Avg) and standard deviation (SD) values of M_1 of the thermo-elastic problem.

Number of objectives		NSGA-II	SPEA-II	CCMOA	COGA-II	CCCOGA-II
2	Avg	0.0206	0.0201	**0.0198**		
	SD	0.0046	0.0078	0.0072		
3	Avg	0.0873	0.0569	0.0524	0.0553	**0.0265**
	SD	0.0371	0.0239	0.0291	0.0393	0.0082
4	Avg	0.1095	0.1597	0.1270	0.0777	**0.0628**
	SD	0.0186	0.0287	0.0221	0.0323	0.0164
5	Avg	0.1941	0.2743	0.1353	0.0872	**0.0573**
	SD	0.0362	0.0692	0.0257	0.0627	0.0265

From values of M_1 of the heat conduction problem in Table 5.7, CCMOA is worse than NSGA-II and SPEA-II, and in the same way, CCCOGA-II is also worse than is predecessor, COGA-II, for the problem with 3-5 objectives. This shows that there is strong coupling among decision variables for this problem. However, for the highest number of objectives, CCMOA is superior to NSGA-II and SPEA-II, and CCCOGA-II is superior to COGA-II by the effectiveness of co-operative co-evolution similar to the linked problems in Chapter IV. By winning score effectiveness in COGA-II and CCCOGA-II, COGA-II is superior to NSGA-II and SPEA-II, and CCCOGA-II is also superior to CCMOA for any numbers of objectives.

From values of M_1 of the linear-elastic and thermo-elastic problems in Table 5.8 and Table 5.9, CCMOA is mostly better than NSGA-II and SPEA-II. Only for the problems with 4 objectives that CCOMOA is marginally worse than NSGA-II. In the same way, CCCOGA-II is also better than COGA-II, for all numbers of objectives. Compared to the heat conduction problem, there is less linkage among decision variables in the linear-elastic and thermo-elastic problems. However, effects of the linkage among decision variables on co-

operative co-evolution for multi-objective continuum topology optimization problem should be further investigated. By the winning score effectiveness in COGA-II and CCCOGA-II, COGA-II is superior to NSGA-II and SPEA-II, and CCCOGA-II is superior to CCMOA, regardless of numbers of objectives.

The simulation results of the comparisons of all employed MOEAs show that the use of winning score can improve MOEA performance for the continuum topology optimization problems with three-or-more objectives. On the other hand, the effectiveness of co-operative co-evolution strategy for multi-objective continuum topology optimization is problem dependent; previously stated, it should be further studies.

5.4.3. Progressive Refinement and Objective Increasing Runs – Results and Discussions

COGA-II is picked for the progressive refinement run (Figure 5.16) for the heat conduction problem with 3 objectives and all 6 objectives in the objective increasing run (Figure 5.18) of which the initial number of objectives is equal to 3 (Table 5.6). For the linear-elastic and thermo-elastic problems, CCMOA is picked for the progressive refinement run for the problems with 2 objectives, and the initial number of objectives, which is equal to 2, in the objective increasing run, while CCCOGA-II is selected for the other numbers of objectives in the objective increasing run.

The selection of MOEAs for the runs is considered by the emperical results of criteria M_1 and CI of benchmark problems in Chapter IV (Table 4.6-Table 4.21) and the results of M_1 (Table 5.7-Table 5.9). In practical, it is not necessary to tested all candidated MOEAs by the criteria. From the empirical results, the employment of winning score in COGA-II and CCCOGA-II can improve the performance of MOEAs for all problems with three-or-more objectives. Although co-operative co-evolution in CCMOA and CCCOGA-II can improve the performance of MOEAs in most employed problems, it is not suitable for some

problems such as the linked DTLZ6 and heat condution problems. Its effectiveness should be further studied. However, a user may know whether it is suitable for a particular problem or not by experience.

Therefore, the selection of MOEAs for an optimization problem can be described as follows. For a problem which the co-operative co-evolution is suitable, CCMOA should be picked for a searching run with only 2 optimized objectives while CCCOGA-II should be picked for a searching run opimizing three-or-more objectives. On the other hand, if the co-operative co-evolution is not suitable, NSGA-II or SPEA-II can be picked in a searching run opimizing 2 objectives while COGA-II should be used for a searching run with three-or-more optimized objectives.

For a continuum topology optimization, objectives of a solution are evaluated by numerical method such as finite element method and finite volume method. The computational time of objective evaluation is then much more than that of MOEA process. Then, total computational time of a search can be indicated by the number of objective evaluations. Since it is hard to reduce the computational time of objective evaluations, a suitable searching run with a good MOEA which can reduce total computational time is necessary. The proposed searching runs – progressive refinement and objective increasing runs – with the suitable selected MOEA can accelerate solutions and reduce the number of objective evalutions in order to reduce the number of objective evalutions and total computational time.

Average computational time on the same computer (a Pentium IV 3.06 GHz processor with 2.00 GB of RAM) of the proposed searching runs for the employed continuum topology optimization problems are displayed in Table 5.10.

The non-dominated solutions of all employed continuum topology optimization problems are as following topics. The objectives of a non-dominated

solution which will be displayed in the following topics are not exact values. They are only tended values, since they are evaluated by coarse mesh due to restriction of time.

Table 5.10 Average computational time of progressive refinement and objective increasing runs of employed continuum topology optimization problems.

Problem		Progressive Refinement Run	Objective Increasing Run
Heat Condution		6.12 minutes	7.58 minutes
Linear-Elastic		109.39 minutes	139.20 minutes
Thermo-Elastic	$T_0 = 10°C$	154.54 minutes	197.18 minutes
	$T_0 = 20°C$	170.64 minutes	211.01 minutes
	$T_0 = 40°C$	182.96 minutes	220.31 minutes

The multiple non-dominated solutions are shown for each employed problem. As previously stated in Chapter II, this thesis will not choose one solution for an employed problem as that in Figure 2.7.

True Pareto-optimal solutions of an employed continuum topology optimization can be obtained by only an exhaustive search. However, due to restriction of time, it is impossible to evaluate objectives of all possible configurations in order to obtain the true Pareto-optimal solutions. The non-domainted solutions which are shown in the following topics may not the true Pareto-optimal solutions, they are only approximated solutions.

1. Heat Conduction Non-dominated Solutions

The non-dominated front with 20 selected non-dominated solutions with temperature (°C) profile in the heating plate and temperature (°C) contours of the selected solutions of the problem with 3 objectives and 6 objectives are shown in Figure 5.20-Figure 5.23. For a structure in Figure 5.20 and Figure 5.22, numbers in the bracket ( ) are corresponding objectives of the structure.

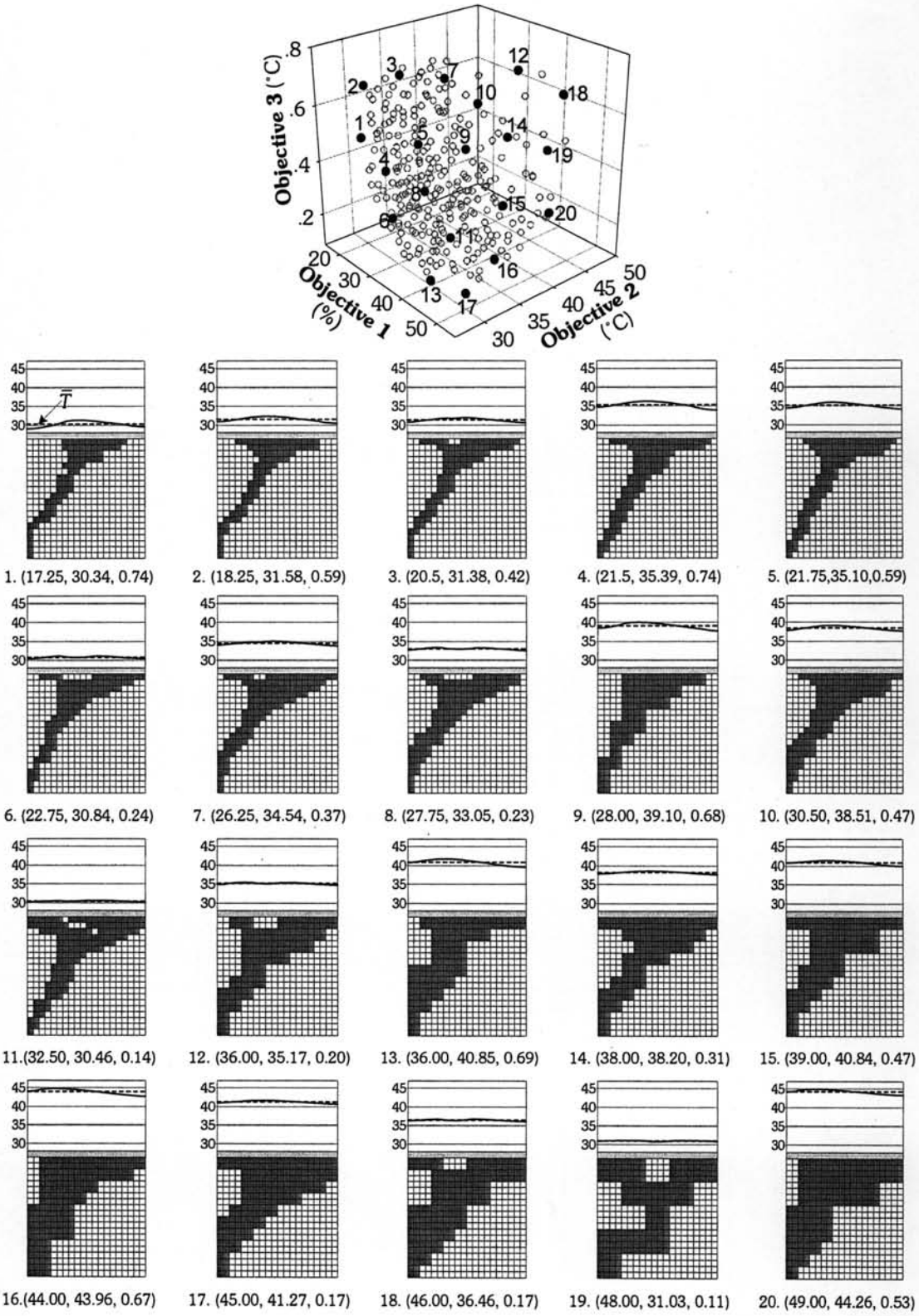

Figure 5.20 Non-dominated front and 20 selected solutions with temperature (°C) profile in the heating plate of the heat conduction problem with 3 objectives (Weight, $\bar{T}$, SD_T).

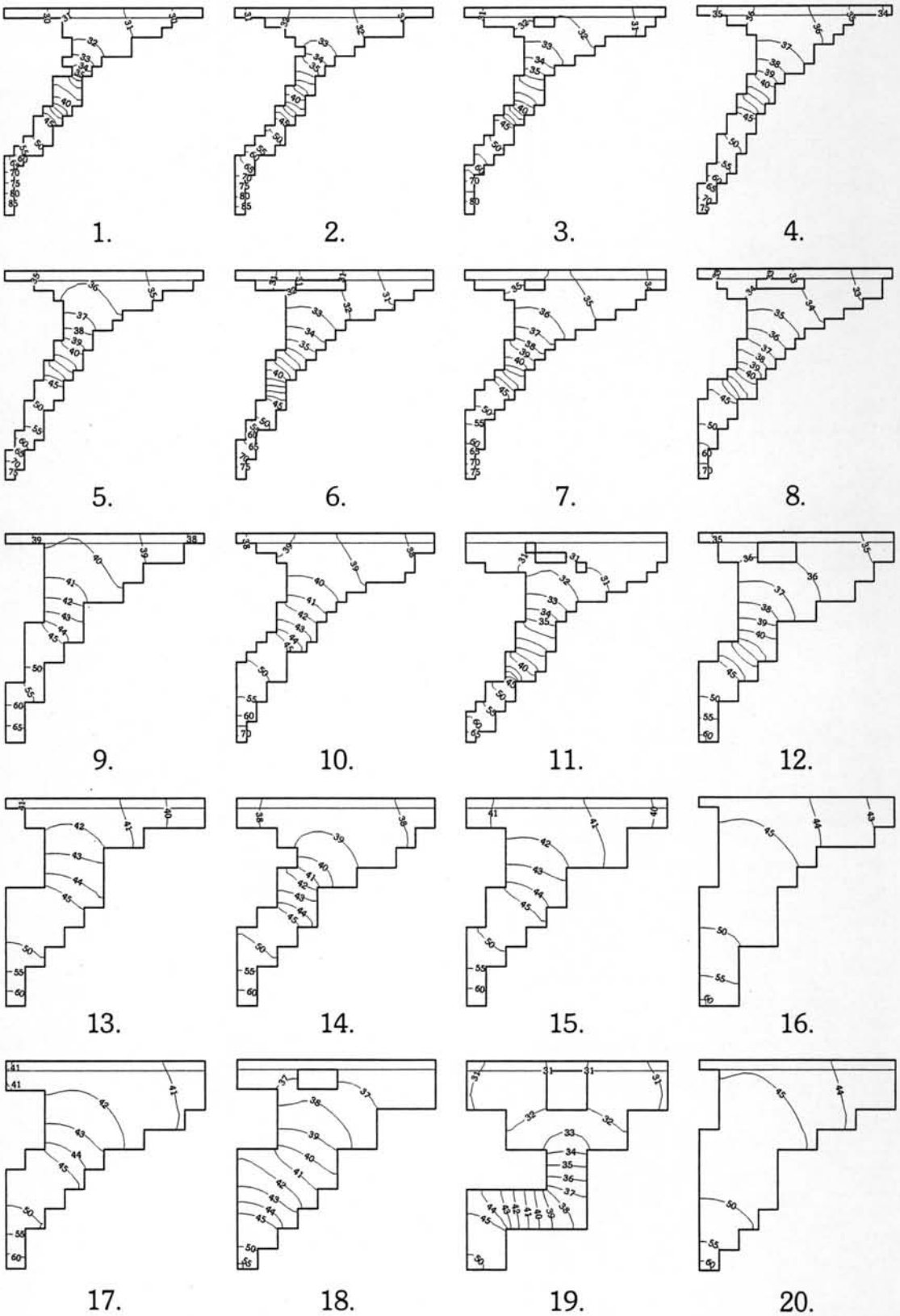

Figure 5.21 Temperature (°C) contours of 20 selected solutions of the heat conduction problem with 3 objectives.

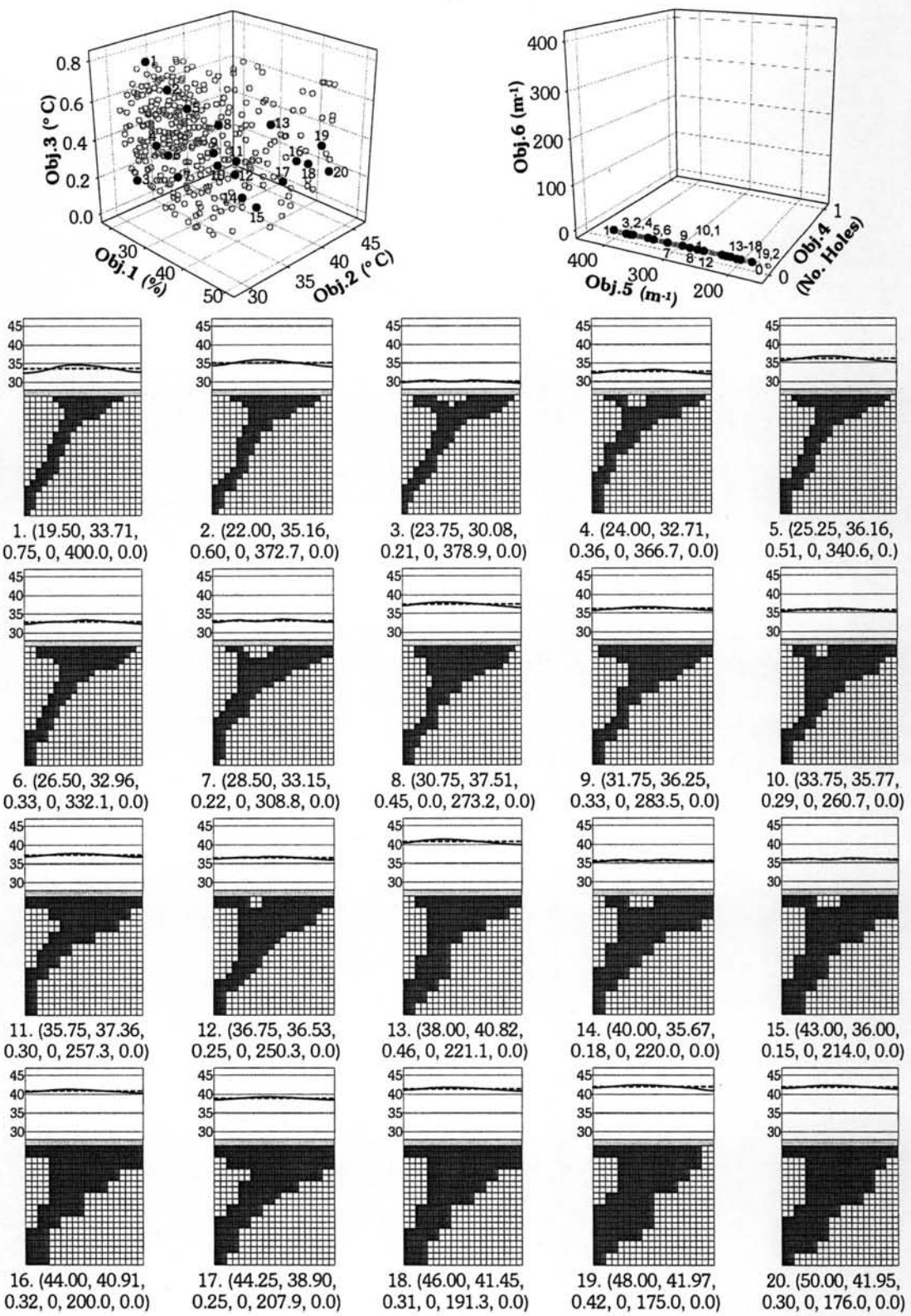

Figure 5.22 Non-dominated front and 20 selected solutions with temperature profile in the heating plate of the heat conduction problem with 6 objectives (Weight, $\overline{T}$, SD_T, No. holes, R_{pa}, MRH_{pa}).

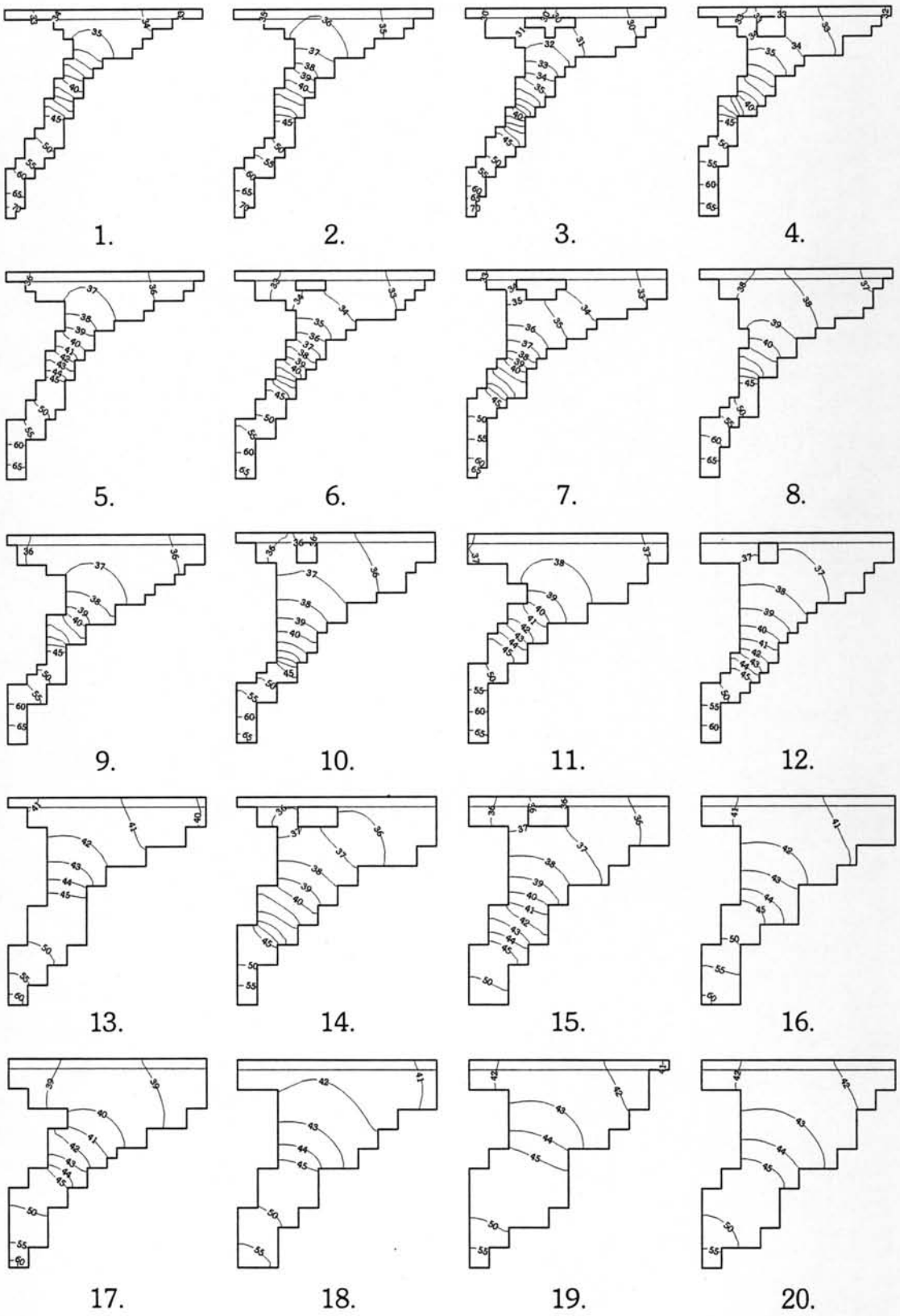

Figure 5.23 Temperature (°C) contours of 20 selected solutions of the heat conduction problem with 6 objectives.

From Figure 5.20 and Figure 5.22, optimized structures transfer heat into middle elements in top rows, and distribute the heat to a plate in order to reduce temperature standard deviation SD_T in the plate. In addition, some structures which are displayed by the numbers 3, 6-8, 11, 12, 18, 19 in Figure 5.20 and 3, 4, 7, 10, 12, 14, 15 in Figure 5.22 have convective surface below middle portion of the plate, in which temperature is higher than other portions, to transfer heat to the surroundings in order to reduce temperature in the portion and the SD_T in the plate.

The obtained solutions in Figure 5.20 and Figure 5.22 are not dominated by two extreme true Pareto-optimal solutions by Pareto domination without goal attainment in Figure 5.5. They are much more useful than the extreme true Pareto-optimal solutions; an objective of the obtained solutions is not very poor as that of the extreme true Pareto-optimal solutions.

By optimizing all design objectives in Figure 5.22, structures with small inside holes such as the eleventh structure in Figure 5.20 and complex structures such as the first structure in Figure 5.20 are eliminated. And also, no structures with inside holes by this optimization are obtained. Compared to structures in Figure 5.20, in overall, the structures in Figure 5.22 are quite simpler than those are obtained by optimizing only 3 basic objectives in Figure 5.20.

2. Linear-Elastic Non-dominated Solutions

After all repeated runs, examples of 12 selected non-dominated solutions and vertical deflection contours of the selected structures for 2 and 5 objectives are shown in Figure 5.24-Figure 5.27. In addition, objectives and vertical deflection contours of 4 solutions – A, B, C, and D – approximated from the optimized solution by the design sensitivity method analyis (DSA) [71] which employs an artificial decoded density decision variable in Figure 5.8(a), are shown in Figure 5.24 and Figure 5.25.

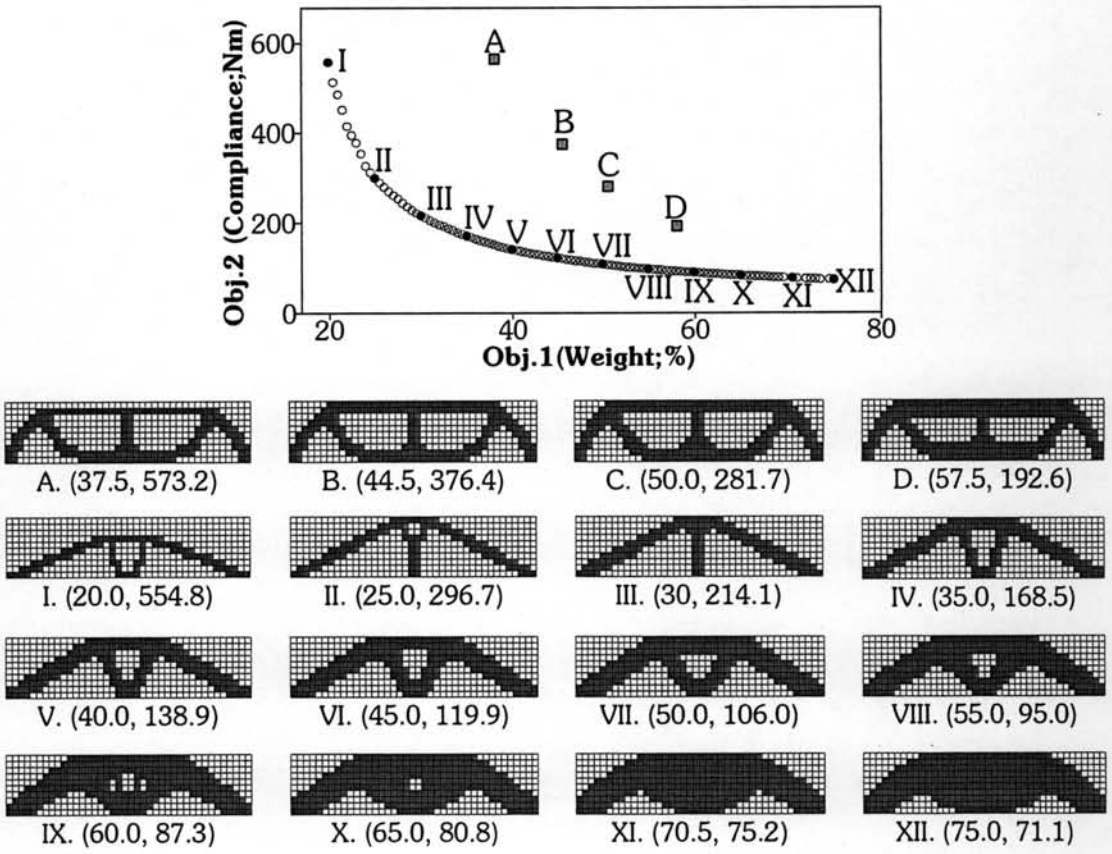

Figure 5.24 Non-dominated front and 12 selected solutions of the linear elastic problem with 2 objectives (Weight, Compliance).

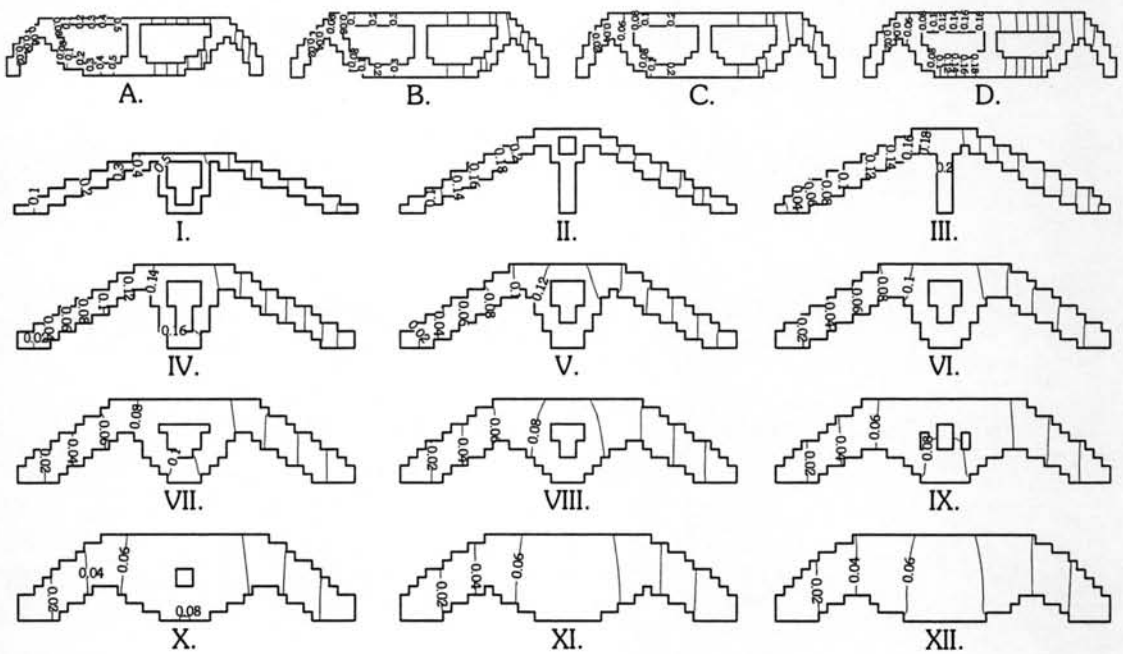

Figure 5.25 Vertical deflection (mm) contours of 12 selected solutions of the linear elastic problem with 2 objectives.

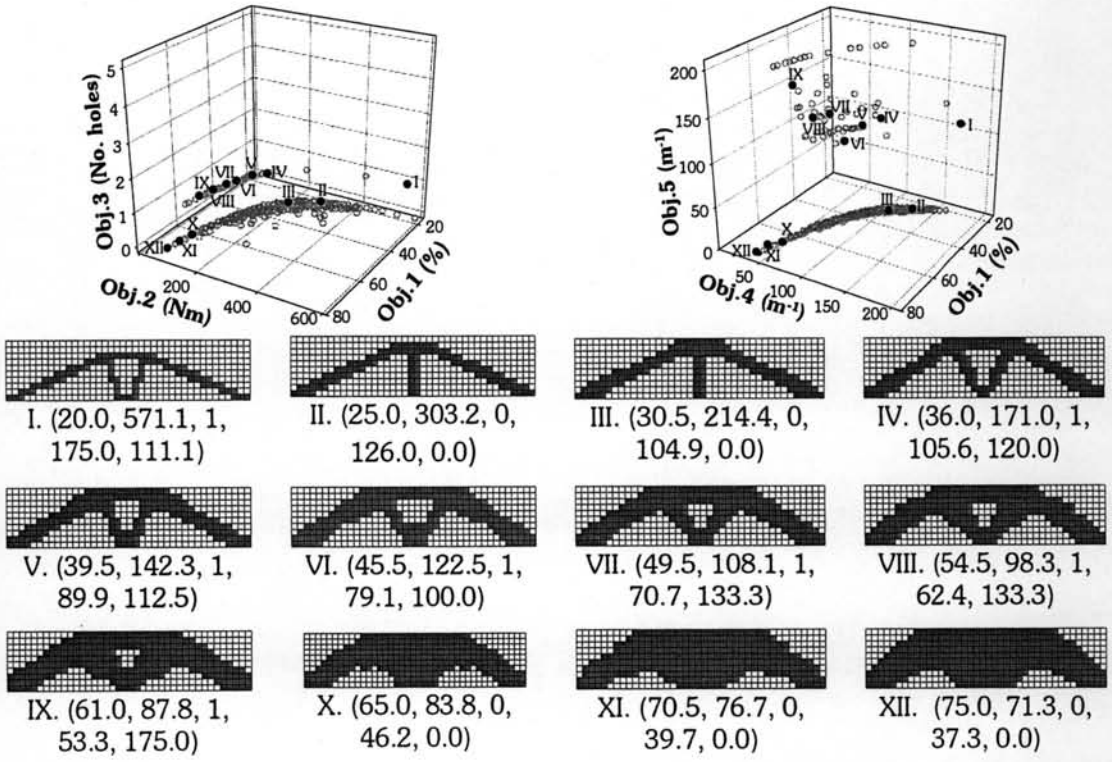

Figure 5.26 Non-dominated front and 12 selected solutions of the linear elastic problem with 5 objectives (Weight, Compliance, No. holes, R_{pa}, MRH_{pa}).

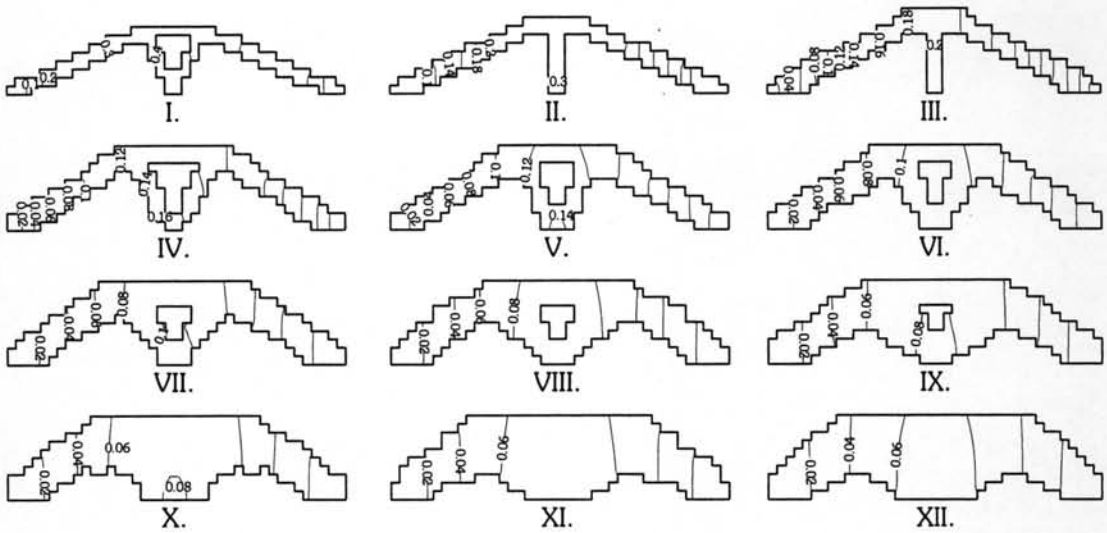

Figure 5.27 Vertical deflection (mm) contours of 12 selected solutions of the linear elastic problem with 5 objectives.

Compared to the previous study [71], the obtained structures are more V-shaped. Since the concentrated force is applied at the middle point of a structure

(Figure 5.6), material elements in the middle portion of the structures can more reduce deflection or compliance than those of other portions. Therefore, the optimized structures in Figure 5.24 and Figure 5.26 have v-shaped material distribution. They are quite different from the structure the structure of the study for the linear-elastic problem in Figure 5.8a. Since they have more material elements material elements in the middle portion, they are better than the structure in Figure 5.8a. This can be described the comparison of solutions obtained by the progressive refinement run with the second proposed MOEA – CCMOA – and 4 approximated solutions – A, B, C, and D – which are evaluated from the solution by design sensitivity analysis method [71] in Figure 5.24. From the graph in Figure 5.24, the obtained solutions are much superior to the approximated solutions.

Similar to the heat conduction problem, the obtained solutions in Figure 5.24 and Figure 5.26 are not dominated by two extreme true Pareto-optimal solutions by Pareto domination without goal attainment of the linear-elastic problem in Figure 5.7. They are much more useful than the extreme true Pareto-optimal solutions; an objective j of the obtained solutions is not very poor such as the second objective, compliance (Π), and the first objective, structural weight, of the first and second known extreme true Pareto-optimal solutions, respectively.

Since the structures by optimizing only 2 objectives are quite simple, then there is little difference between in Figure 5.24, and those by optimizing all design objectives in Figure 5.26.

3. Thermo-Elastic Non-dominated Solutions

After all repeated runs, examples of 12 selected non-dominated solutions, deflection and temperature contours of the selected solutions of the problems with 2 and 5 objectives for all 3 values of T_0 – 10°C, 20°C, and 40°C – are shown in Figure 5.28-Figure 5.43. Since optimized solutiond for T_0 = 40°C have no elememts that contact to temperature boundary surface in, then there are no

thermal load for this value of T_0. Temperature contours of the selected solutions of only 2 values of T_0 – 10°C, 20°C – are shown.

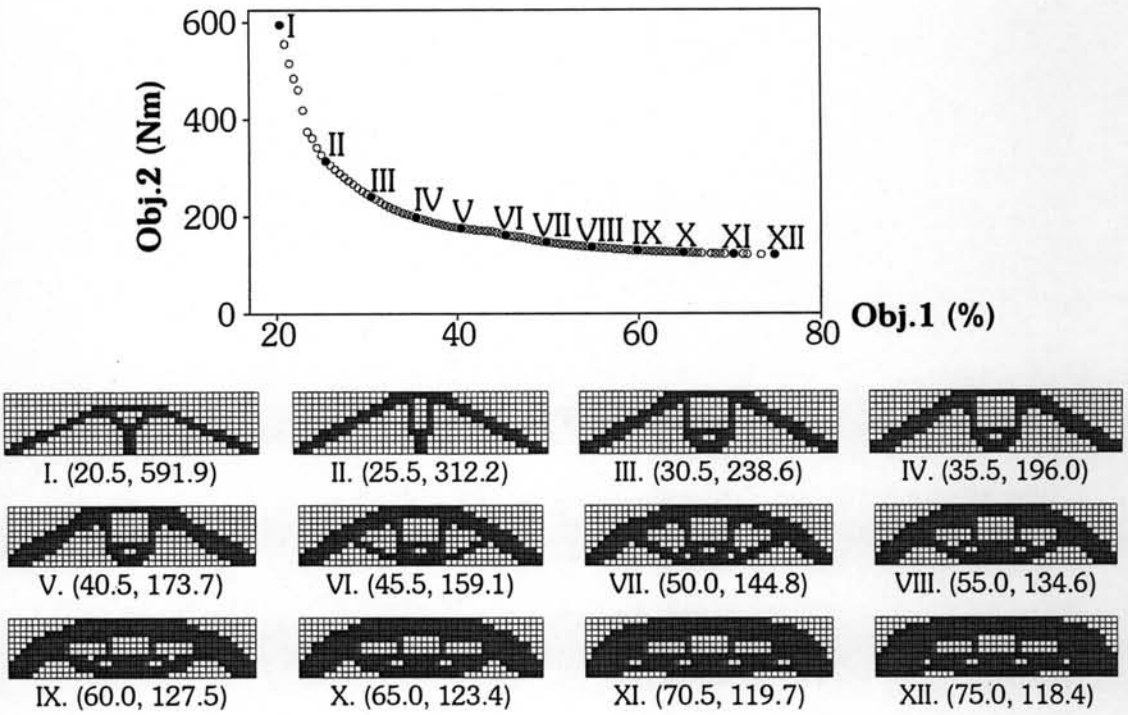

Figure 5.28 Non-dominated front and 12 selected solutions of the thermo-elastic problem with 2 objectives for T_0 = 10°C.

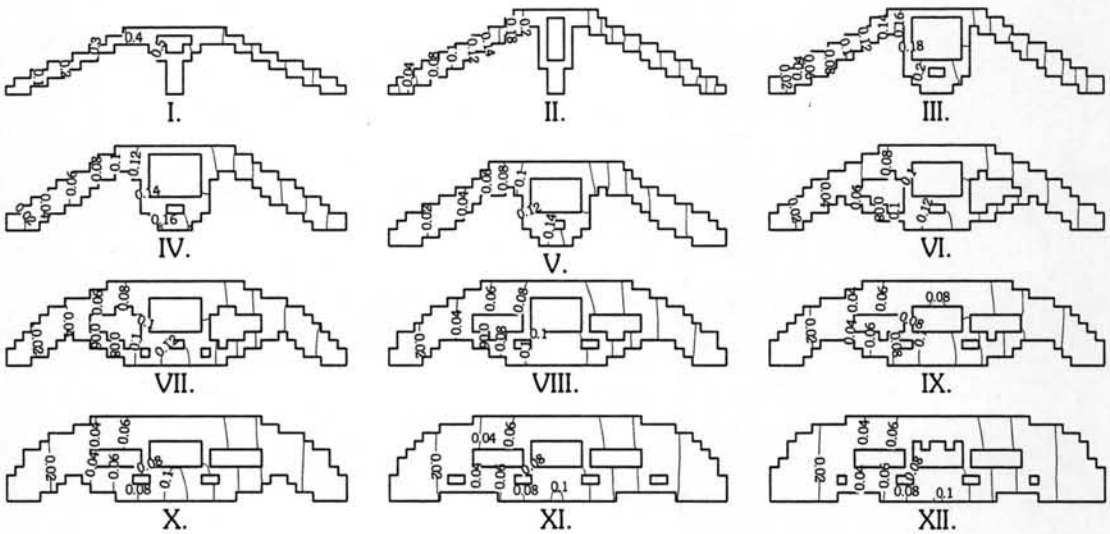

Figure 5.29 Vertical deflection (mm) contours of 12 selected solutions of the thermo-elastic problem with 2 objectives for T_0 = 10°C.

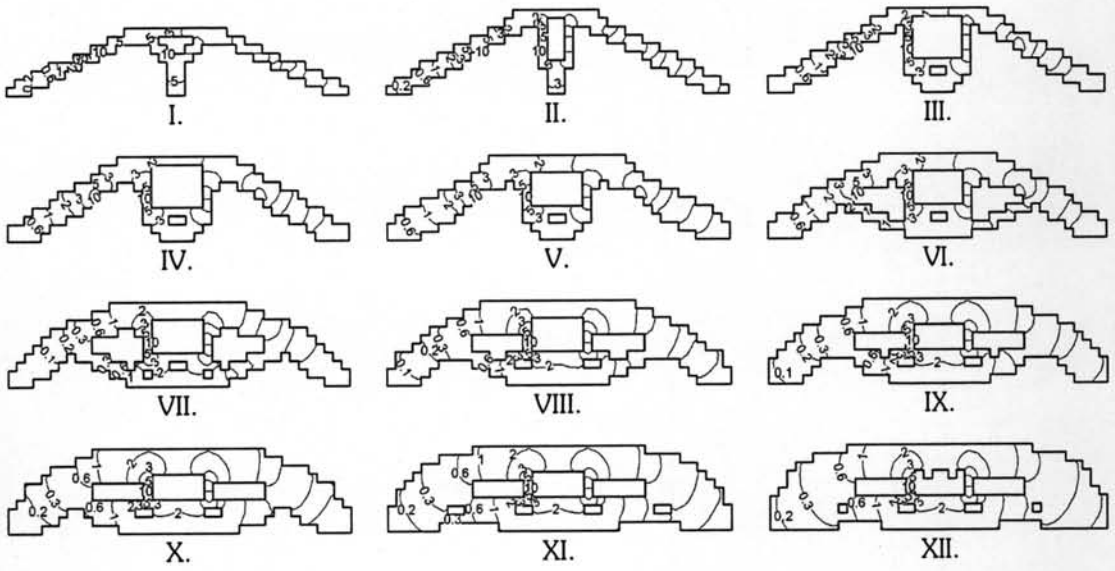

Figure 5.30 Temperature (°C) contours of 12 selected solutions of the thermo-elastic problem with 2 objectives for $T_0 = 10°C$.

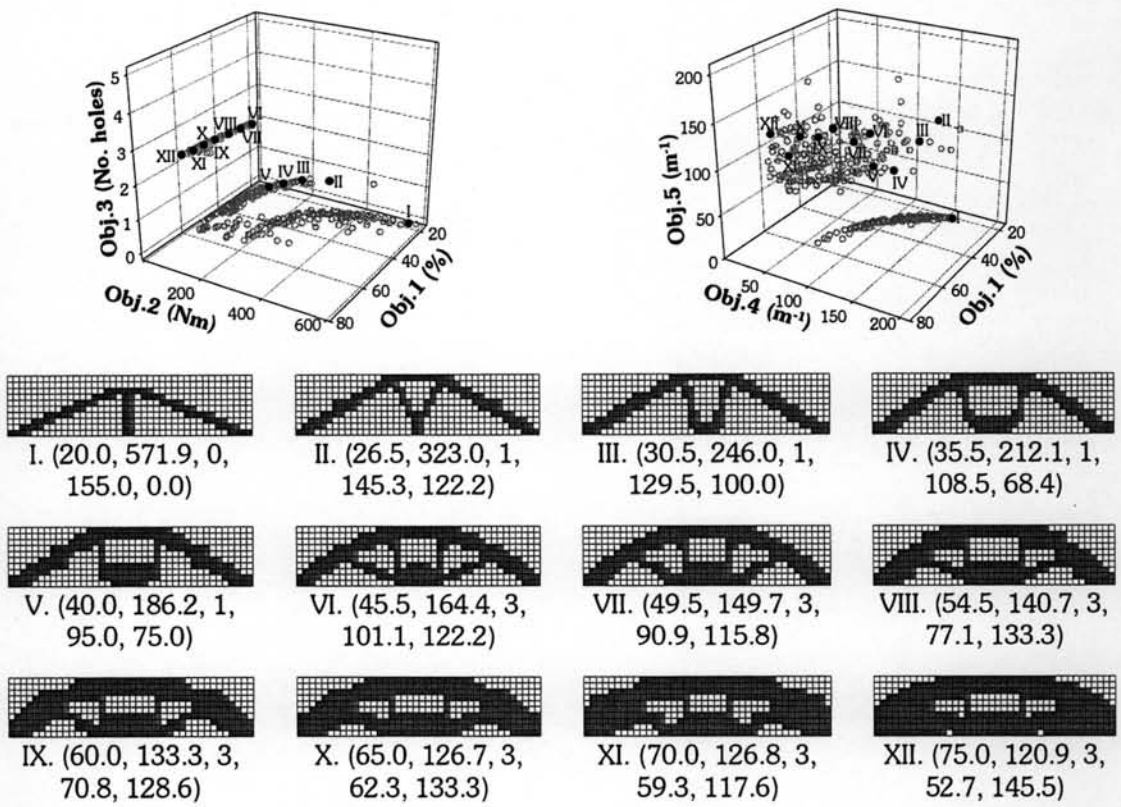

Figure 5.31 Non-dominated front and 12 selected solutions of the thermo-elastic problem with 5 objectives for $T_0 = 10°C$.

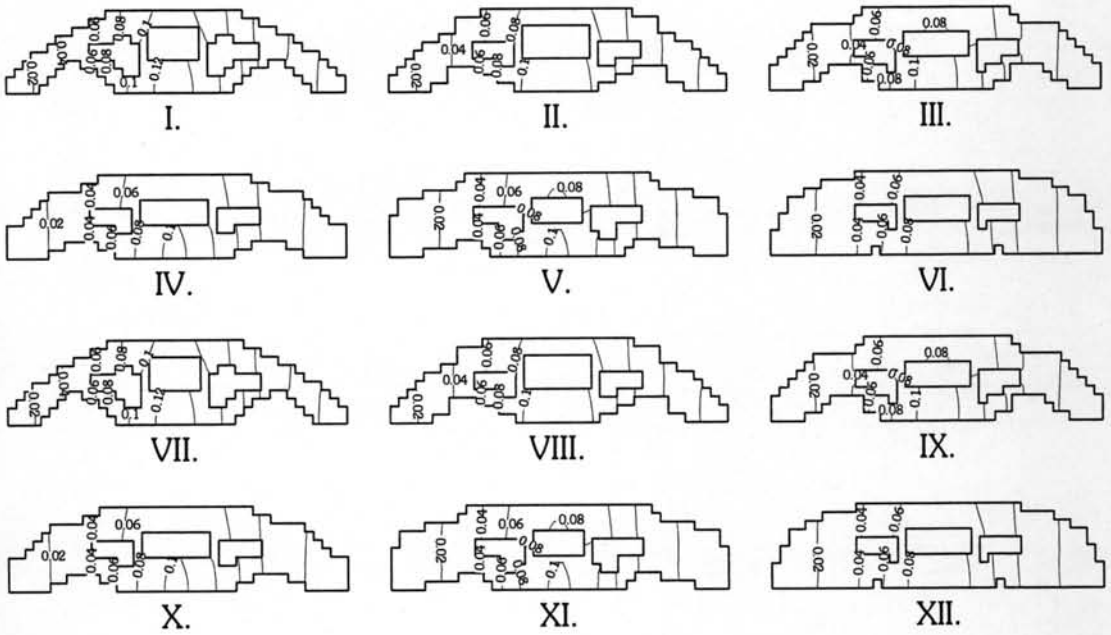

Figure 5.32 Vertical deflection (mm) contours of 12 selected solutions of the thermo-elastic problem with 5 objectives for $T_0 = 10°C$.

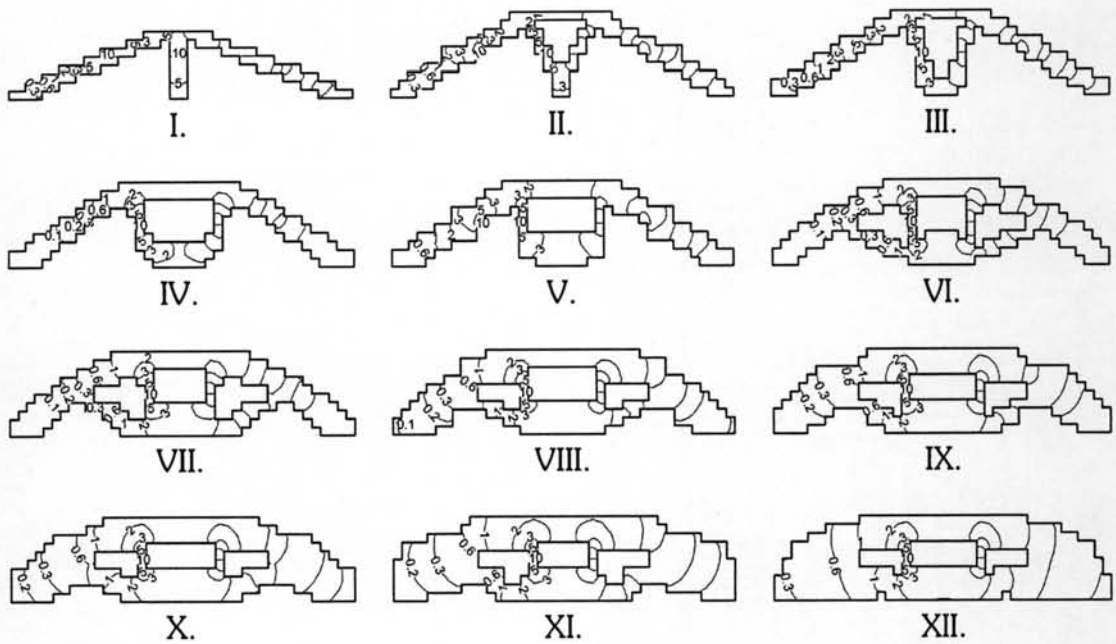

Figure 5.33 Temperature (°C) contours of 12 selected solutions of the thermo-elastic problem with 5 objectives for $T_0 = 10°C$

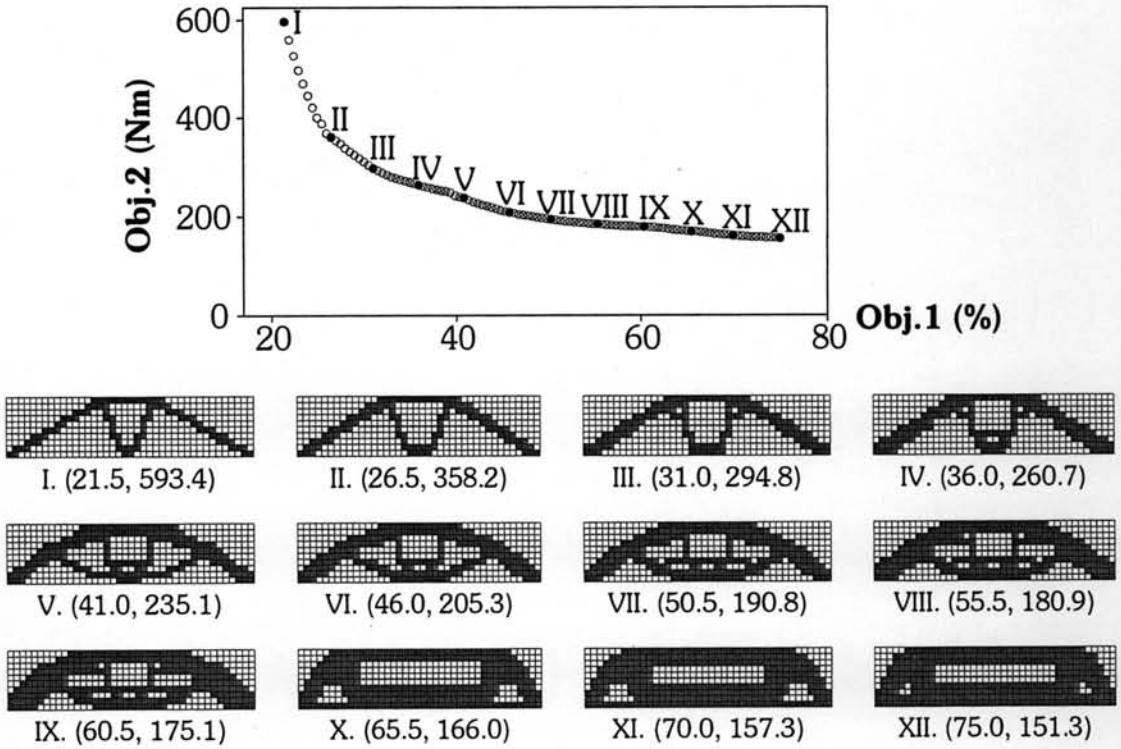

Figure 5.34 Non-dominated front and 12 selected solutions of the thermo-elastic problem with 2 objectives for $T_0 = 20°C$.

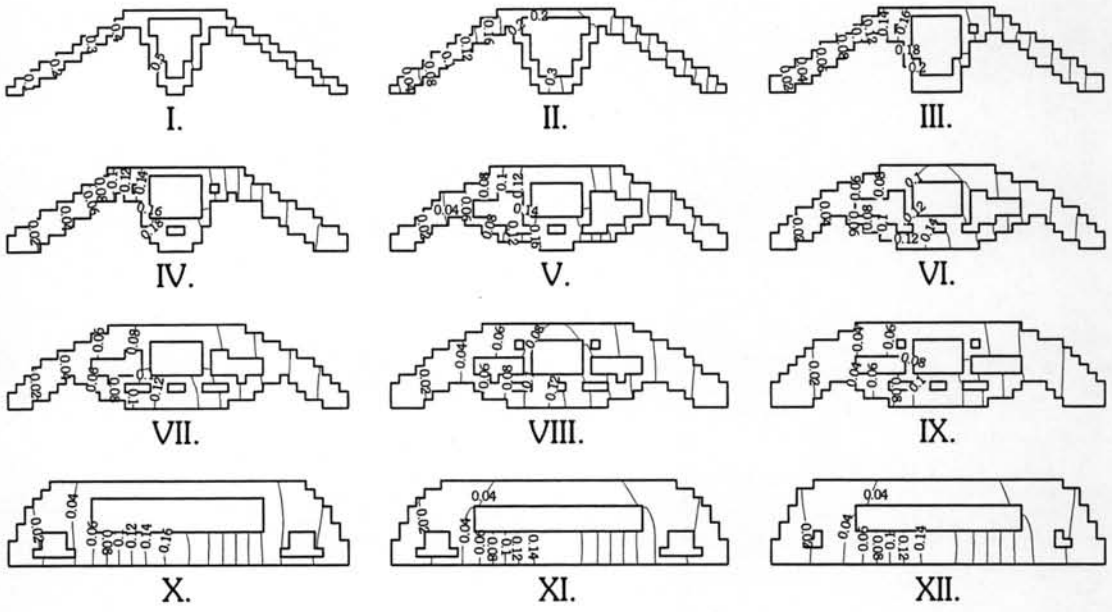

Figure 5.35 Vertical deflection (mm) contours of 12 selected solutions of the thermo-elastic problem with 2 objectives for $T_0 = 20°C$.

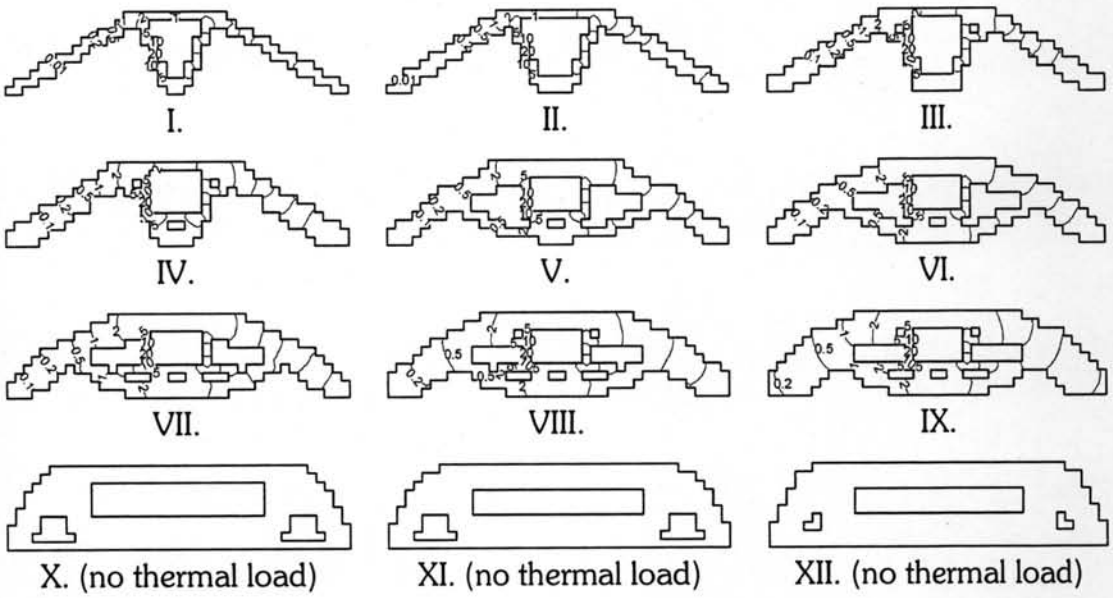

Figure 5.36 Temperature (°C) contours of 12 selected solutions of the thermo-elastic problem with 2 objectives for $T_0 = 20°C$.

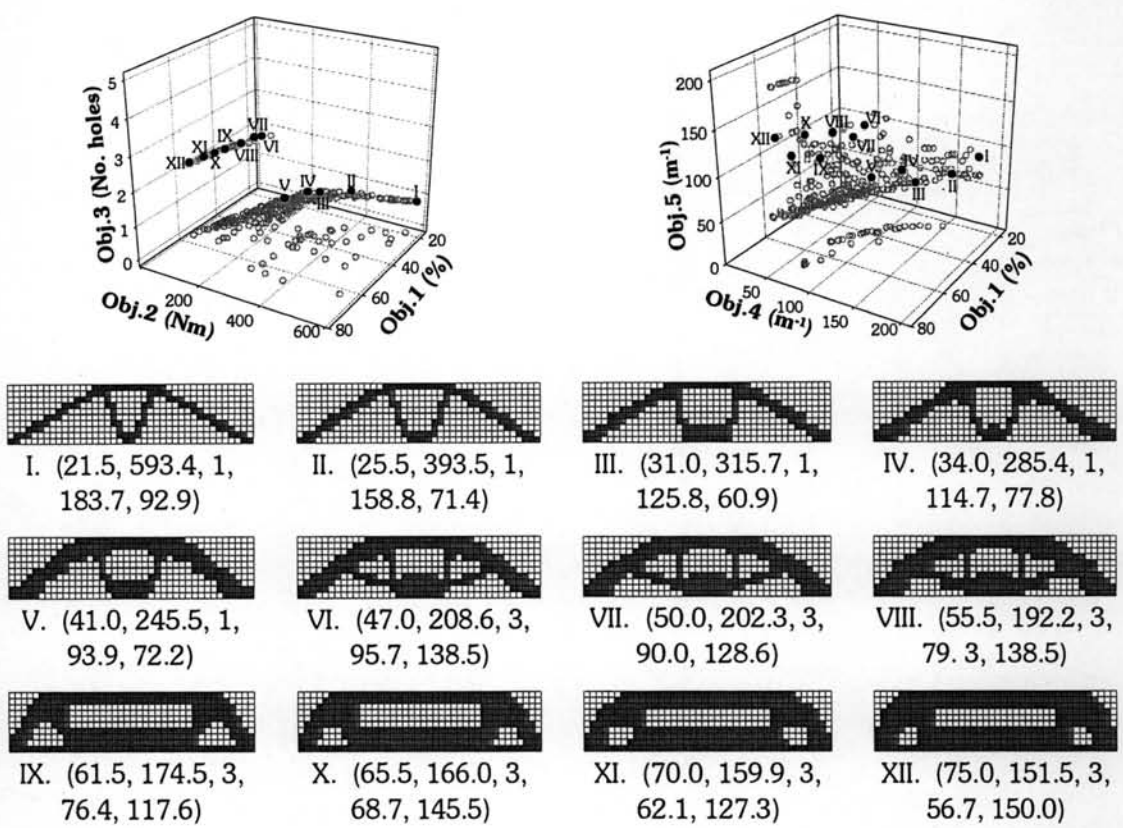

Figure 5.37 Non-dominated front and 12 selected solutions of the thermo-elastic problem with 5 objectives for $T_0 = 20°C$.

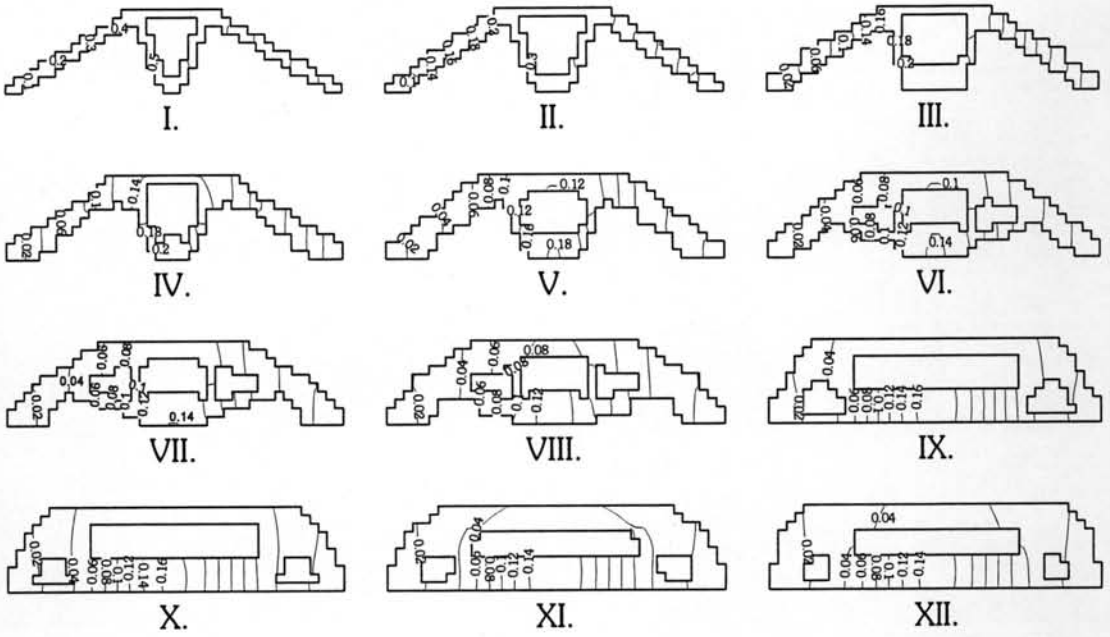

Figure 5.38 Vertical deflection (mm) contours of 12 selected solutions of the thermo-elastic problem with 5 objectives for $T_0 = 20°C$.

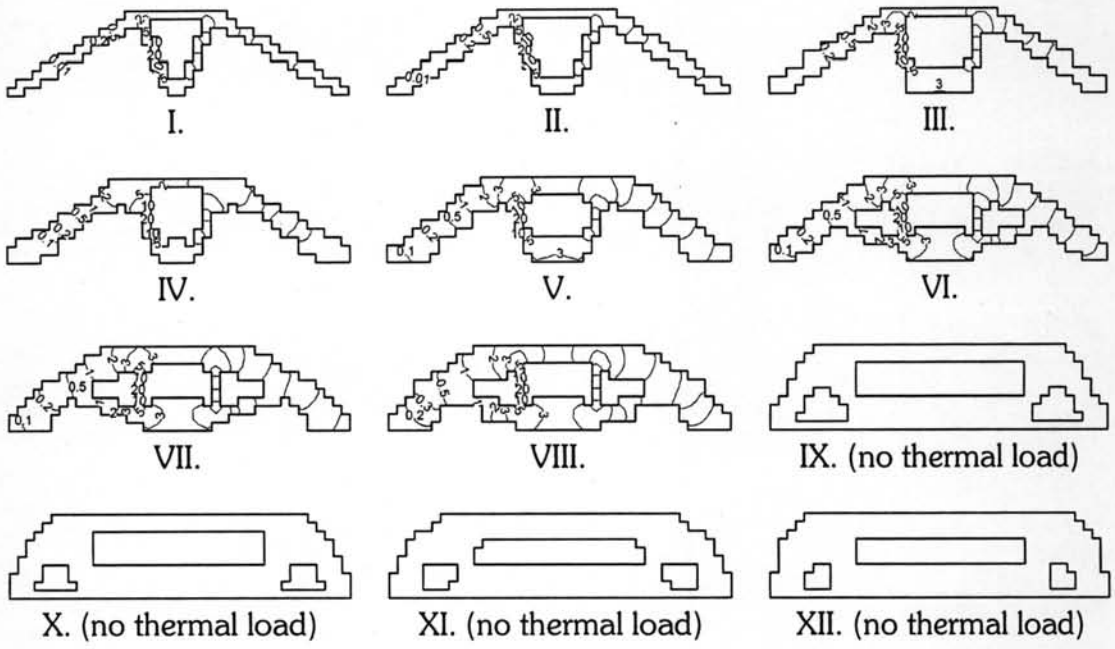

Figure 5.39 Temperature (°C) contours of 12 selected solutions of the thermo-elastic problem with 5 objectives for $T_0 = 20°C$.

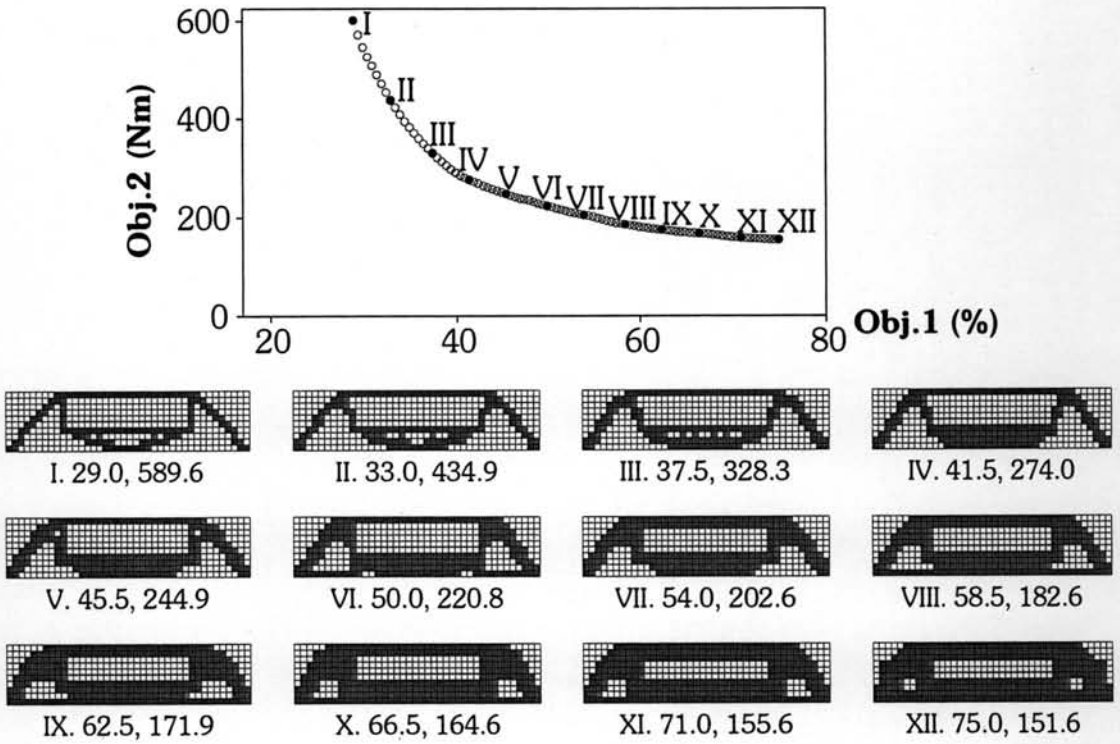

Figure 5.40 Non-dominated front and 12 selected solutions of the problem with 2 objectives for $T_0 = 40°C$.

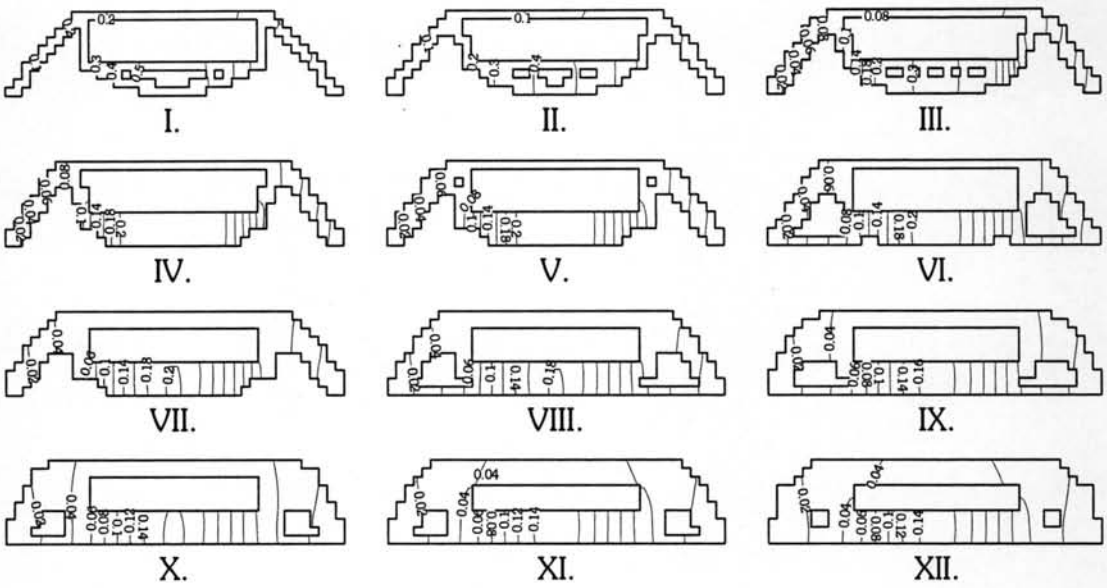

Figure 5.41 Vertical deflection (mm) contours of 12 selected solutions of the thermo-elastic problem with 2 objectives for $T_0 = 40°C$.

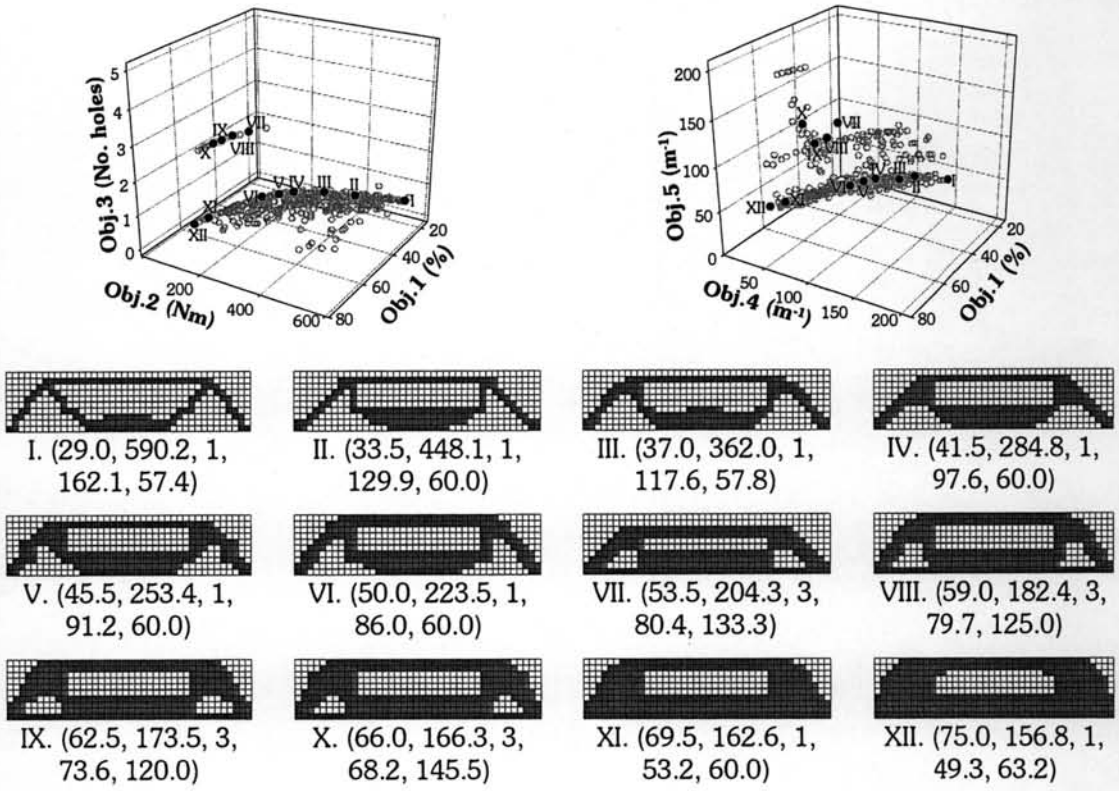

Figure 5.42 Non-dominated front and 12 selected solutions of the problem with 5 objectives for $T_0 = 40°C$.

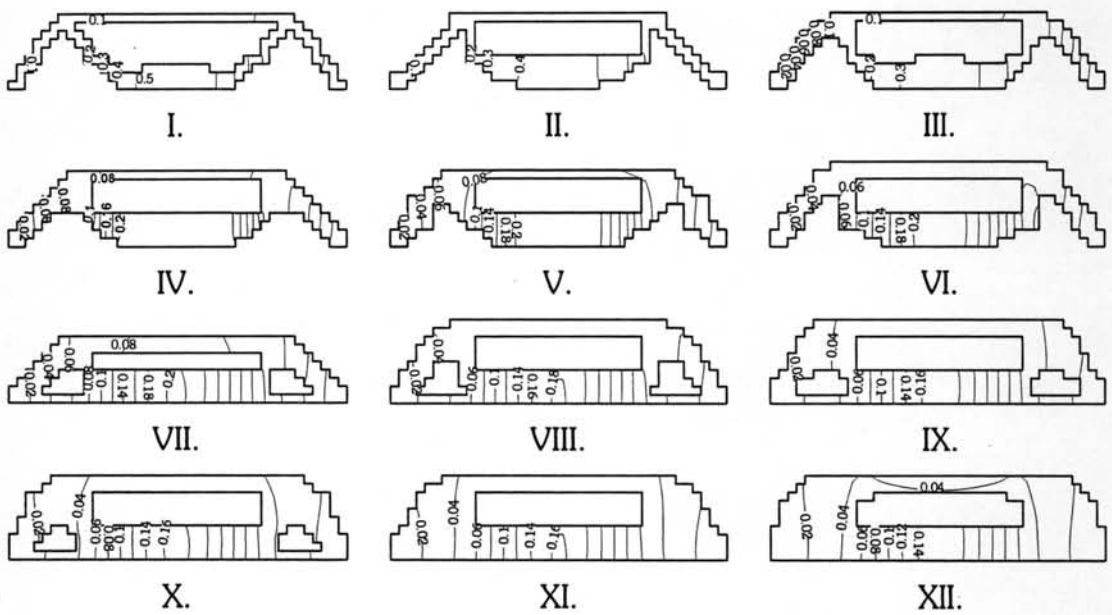

Figure 5.43 Vertical deflection (mm) contours of 12 selected solutions of the thermo-elastic problem with 5 objectives for $T_0 = 40°C$.

The material distribution of optimized structures for all three values of T_0 in Figure 5.28-Figure 5.42 can be described as follows.

Similar to the linear-elastic problem, the optimized structure in for the problem with $T_0 = 10°C$ also have material elements in middle portion of the optimized structures, which reduce the vertical displacement at the applied load point, in order to reduce the mechanical compliance. However, the optimized structures have only a few elements in the middle portion that contact the temperature boundary surface (Figure 5.6) to avoid the thermal loading as much as possible in order to reduce the thermal compliance. In addition, the optimized structures have more convective area to transfer heat from the temperature surface in order to reduce their thermal compliances.

For $T_0 = 20°C$, material distributions of optimized structures of which weight is less than 65% of the domain are similar to those for $T_0 = 10°C$. However, since thermal compliance, which is represented by the first term in equation (5.3), is an integral over structural volume. The thermal compliance of a structure is equal to the summation of thermal compliance of all material elements of the structure. For any 2 structures with similar average temperatures in entire material regions, average thermal compliance densities of the structures are then closed to each other. However, since thermal compliance of a structure is equal to the summation of thermal compliance of all material elements, the thermal compliance of the structure with more material region area or volume is more than that of the other. In addition, since a structure with high weight has many material elements which can reduce vertical deflection at applied force location. Then, impact of mechanical loading tend to decrease while that of thermal tend to increase, when structural weight is more. Therefore, due to higher thermal loading of $T_0 = 20°C$, a high-weight structure has much more thermal compliance than that of the problem with $T_0 = 10°C$, the thermal loading exerts more impact than the mechanical loading. Elements contacting temperature surface of the structure are eliminated in order to vanish thermal compliance.

Similar to the high-weight structure for $T_0 = 20°C$, thermal loading has much more impact than mechanical loading for the highest temperature, $T_0 = 40°C$. Therefore, to avoid any thermal loading, and be subjected to only mechanical loading, all optimized structures in Figure 5.40 and Figure 5.42 do not have elements contacting the temperature surface. In addition, due to this avoidance, a optimized structures have many material elements in the middle bottom portion in order to reduce the mechanical compliance which is the total structural compliance.

Compared to the previous study [71], for $T_0 = 10°C$ and $20°C$, the material of the obtained structures with weight of about 30% of the domain is distributed in V-shape which is similar to the solution of the previous study in Figure 5.8(b). Then, at this weight, the mechanical loading exerts more impact than the thermal loading for these temperatures. On the other hand, the thermal loading has more impact than the mechanical loading for $T_0 = 40°C$; the material of the obtained structures with weight of about 30% of the domain is similar to the solution of the previous study in Figure 5.8(c). Thus, the optimized structures which are obtained from the progressive refinement and objective increasing runs by the proposed MOEAs in Figure 5.20-Figure 5.42 are reliable.

The obtained solutions in Figure 5.24, Figure 5.26, Figure 5.28, Figure 5.31, Figure 5.34, Figure 5.37, Figure 5.40, and Figure 5.42 are not dominated by only one known extreme true Pareto-optimal solutions by Pareto domination without goal attainment for any values of T_0 in Figure 5.7a. They are much more useful than the extreme true Pareto-optimal solutions; an objective j of the obtained solutions is not very poor such as the second objective, compliance (Π), of the known extreme true Pareto-optimal solution.

By optimizing all 5 design objectives including 3 geometrically structural objectives, the obtained structures are quite simpler than those are obtained by optimizing only 2 basic objectives. In addition, optimized structures with many

small holes, such as optimized structures for T_0 = 10°C in Figure 5.28, T_0 = 20°C in Figure 5.34, and light-weight structures for T_0 = 40°C in Figure 5.40, are replaced by the optimized structures with a few large holes. For example, by optimizing all design objectives, the seventh optimized structure, which is obtained by optimizing only 2 basic objectives of the thermo-elastic problem with T_0 = 10°C, in Figure 5.28 is replaced by the seventh optimized structure in Figure 5.31. Although by considering only 2 basic objectives, the optimized structure from Figure 5.31, is marginally worse than that from Figure 5.28; it is simpler and much easier for further detailed design such as shape design.

5.5. Closing Remarks

From the simulation results of this chapter, proposed MOEAs – CCMOA, COGA-II, and CCCOGA-II – are better than NSGA-II and SPEA-II. This shows that the proposed MOEAs can improve performances of MOEAs not only for benchmark problems, but also for continuum topology optimization problems, which are real-world problems. They can also search for reliable solutions for the continuum topology optimization problems. Due to the previously stated weak point of a sensitivity analysis method of the previous study [71] and solutions comparison in the linear-elastic problem in Figure 5.24, the proposed MOEAs are therefore more suitable for continuum topology optimization problems.